including high serum IgG4 level, IgG4-positive plasmacytic infiltration, and fibrosis.

Conversely, CD40, CD154, B-cell activating factor belonging to the tumor necrosis factor family (BAFF), a proliferation-inducing ligand (APRIL), interferon regulatory factor 4 (IRF4), activation-induced cytidine deaminase (AID), and IL-21 contribute to nonspecific immunoglobulin class-switch recombination (from IgM to IgG1, IgG2, IgG3, IgG4, IgA, and IgE) [12-14], as well as IL-4, IL-13, IL-10, and TGF-β. The roles of these nonspecific immunoglobulin class switch-related molecules in the pathogenesis of IgG4-RD have not been reported previously.

To determine the mechanism of upregulation of IgG4 class-switch recombination in IgG4-RD, the mRNA expression levels of IgG4-specific and nonspecific class switch-related molecules were first measured in peripheral blood mononuclear cells (PBMCs), CD3-positive T cells, and CD20-positive B cells sorted from PBMCs, as well as labial salivary glands (LSGs) of IgG4-RD. Then, these levels were compared with those measured in patients with Sjögren syndrome (SS) and in healthy controls.

## Materials and methods

### Study population

PBMC samples were collected from six Japanese patients with IgG4-RD, as well as from six Japanese patients with SS who had been followed up at the University of Tsukuba Hospital (Ibaraki, Japan). LSG samples were also collected from 11 Japanese patients with IgG4-RD and 13 Japanese patients with SS who had been followed up at the University of Tsukuba Hospital and Kyushu University Hospital (Fukuoka, Japan). All patients with IgG4-RD satisfied the comprehensive diagnostic criteria for IgG4-related disease (IgG4-RD) 2011 proposed by the All Japan IgG4 team [15]. The diagnosis of IgG4-RD was based on the presence of all three items: (1) clinical examination showing characteristic diffuse/localized swelling or masses in single or multiple organs, (2) hematologic examination showing elevated serum IgG4 concentrations (135 mg/dl), and (3) histopathologic examination showing (a) marked lymphocyte and plasmacyte infiltration and fibrosis; (b) infiltration of $IgG4^+$ plasma cells: ratio of $IgG4^+/IgG^+$ cells >40% and >10 $IgG4^+$ plasma cells/HPF. All patients with SS satisfied the Japanese Ministry of Health criteria for the diagnosis of SS (1999) [16]. These criteria included four clinicopathologic findings: lymphocytic infiltration of the salivary or lacrimal glands, dysfunction of salivary secretion, keratoconjunctivitis sicca, and presence of anti-SS-A or -SS-B antibodies. The diagnosis of SS was based on the presence of two or more of these four items. We also collected control samples: PBMCs from eight and LSGs from three healthy subjects. Approval for this study was obtained from the local ethics committee, and a signed informed consent was obtained from each subject.

### Sorting of CD3-positive T cells and CD20-positive B cells from PBMCs with flow cytometry

PBMCs derived from IgG4-RD ($n$ = 3), SS ($n$ = 4), and controls ($n$ = 4) were stained with anti-CD3 antibody conjugated with FITC (BioLegend, San Diego, CA, USA) and anti-CD20 antibody conjugated with APC (BioLegend). Stained PBMCs were analyzed and sorted with flow cytometry.

### Analysis of mRNA expression levels of IgG4-specific and nonspecific class switch-related molecules in PBMCs and LSGs

Total RNA was extracted from PBMCs, CD3-positive T cells, and CD20-positive B cells sorted from PBMCs, as well as LSGs, by the ISOGEN method, and cDNA was synthesized by a cDNA synthesis kit (Takara, Otsu, Shiga, Japan). The mRNA expression levels of IgG4-specific class switch-related molecules, such as Th2 cytokines (IL-4 and IL-13), Treg cytokines (IL-10 and TGF-β), and transcriptional factors (GATA3 and Foxp3) were examined with quantitative PCR. IgG4-nonspecific class switch-related molecules, such as CD40, CD154, BAFF, APRIL, IRF4, and AID also were examined. The human glyceralaldehyde-3-phosphate dehydrogenase (GAPDH) was examined as an internal control.

### Statistical analysis

Differences between groups were examined for statistical significance by using the Mann-Whitney $U$ test, whereas differences in frequencies were analyzed with the Fisher Exact probability test. A $P$ value less than 0.05 denoted the presence of a statistically significant difference.

## Results

### Clinical and pathologic features of patients and controls

Table 1 summarizes the clinical and pathologic features of participating subjects. The frequencies of anti SS-A antibodies and anti SS-B antibodies were significantly lower in IgG4-RD than in SS ($P < 0.05$; Fisher Exact probability test). CH50 levels were also significantly lower in IgG4-RD than in SS ($P < 0.05$, Mann-Whitney $U$ test). Table 2 shows material sampling and organ involvements in patients with IgG4-RD. All LSG samples used in this study satisfied histopathologic findings of the comprehensive diagnostic criteria for IgG4-related disease (IgG4-RD) proposed in 2011 by the All Japan IgG4 team [15]. As shown in Table 2, seven of 15 IgG4-RD patients showed salivary and lacrimal glands involvement alone, whereas the others had multiple organ involvements.

**Table 1 Clinical and pathologic features of patients and controls**

| Parameter | IgG4-RD ($n$ = 15) | SS ($n$ = 16) | HC ($n$ = 10) |
|---|---|---|---|
| Age (years) | 62.9 ± 10.5[a] | 55.9 ± 15.7[a] | 40.9 ± 17.1 |
| Sex (males/females) | 6/9 | 2/14 | 5/5 |
| Anti-SS-A antibody (%) | 0[b] | 93.8 | n.d. |
| Anti-SS-B antibody (%) | 0[b] | 56.3 | n.d. |
| Serum IgG4 (mg/dl) | 942.2 ± 612.5 | n.d | n.d. |
| Serum IgE (U/ml) | 294.0 ± 317.8 | n.d | n.d. |
| CH50 (U/ml) | 33.6 ± 17.5[b] | 50.6 ± 16.3 | n.d. |
| IgG4/IgG in LSG (%) | 62.0 ± 3.5 | n.d | n.d. |

Data are expressed as mean ± SD. n.d., not determined. [a]$P < 0.05$, compared with the healthy control subjects (Mann-Whitney $U$ test or Fisher Exact probability test). [b]$P < 0.05$, compared with the SS group (Mann-Whitney $U$ test or Fisher Exact probability test).

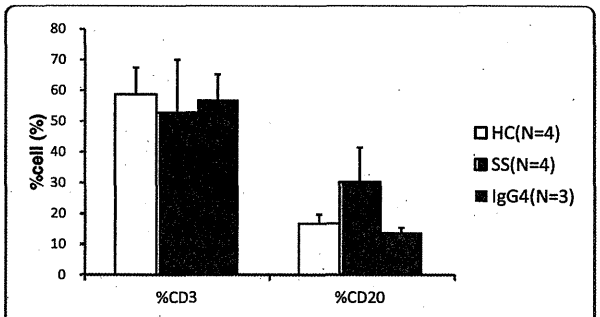


**Figure 1 The cell population of CD3-positive T cells and CD20-positive B cells in peripheral blood mononuclear cells.** PBMCs stained with anti-CD3 antibody and anti-CD20 antibody were analyzed and sorted with flow cytometory. HC, healthy control; SS, Sjögren syndrome; IgG4, IgG4-RD.

### The cell population of CD3-positive T cells and CD20-positive B cells in PBMCs

Figure 1 shows the cell population of CD3-positive T cells and CD20-positive B cells sorted from PBMCs of patients with IgG4-RD ($n$ = 3), SS ($n$ = 4), and the control ($n$ = 4). The population of CD20-positive B cells in SS was higher than the others (no statistically significant difference), whereas that of CD3-positive T cells was comparable in the three groups.

### The mRNA expression levels of IgG4-specific class switch-related molecules in PBMCs, CD3-positive T cells, and CD20-positive B cells in PBMCs and LSGs

Figure 2 shows the mRNA expression levels of IgG4-specific class switch-related molecules in PBMCs and LSGs. The mRNA expression level of IL-4 was significantly higher in LSGs of IgG4-RD than in the control ($P < 0.05$, Mann-Whitney $U$ test). Treg cytokines (IL-10 and TGF-β) were significantly higher in LSGs of IgG4-RD than SS and control ($P < 0.05$, each, Mann-Whitney $U$ test). No significant differences were noted in the PBMC expression levels of various cytokines, among the three groups. In LSGs, the expression of GATA3 was significantly lower in IgG4-RD than in SS; Foxp3 was significantly higher in IgG4-RD and SS than in the control ($P < 0.05$; Mann-Whitney $U$ test). However, no statistically significant difference in Foxp3 expression level was seen between IgG4-RD and SS.

No significant differences were seen in the expression levels of various IgG4-specific class switch-related molecules in CD3-positive T cells and CD20-positive B cells

**Table 2 Material sampling and organ involvements in patients with IgG4-RD**

| Case | Material sampling | | | Organ involvement |
|---|---|---|---|---|
| | PBMC | CD3/CD20 | LSG[a] | |
| 1 | o | | o | MD, lymph node, lung |
| 2 | o | | o | MD, lymph node |
| 3 | o | o | | MD |
| 4 | o | | | MD, lymph node |
| 5 | | | o | MD, lung |
| 6 | o | o | | MD, lymph node, para-aorta swelling |
| 7 | o | o | | Intraorbital mass, retroperitoneal fibrosis |
| 8 | | | o | MD |
| 9 | | | o | MD |
| 10 | | | o | MD |
| 11 | | | o | MD |
| 12 | | | o | MD |
| 13 | | | o | MD |
| 14 | | | o | MD, lung |
| 15 | | | o | MD, liver |

PBMCs, peripheral blood mononuclear cells; CD3/CD20, CD3-positive T cells and CD20-positive B cells sorted from PBMCs; LSG, labial salivary gland; MD, Mikulicz disease (salivary and lacrimal glands). [a]All LSG samples satisfied histopathologic findings of the comprehensive diagnostic criteria for IgG4-related disease (IgG4-RD) 2011.

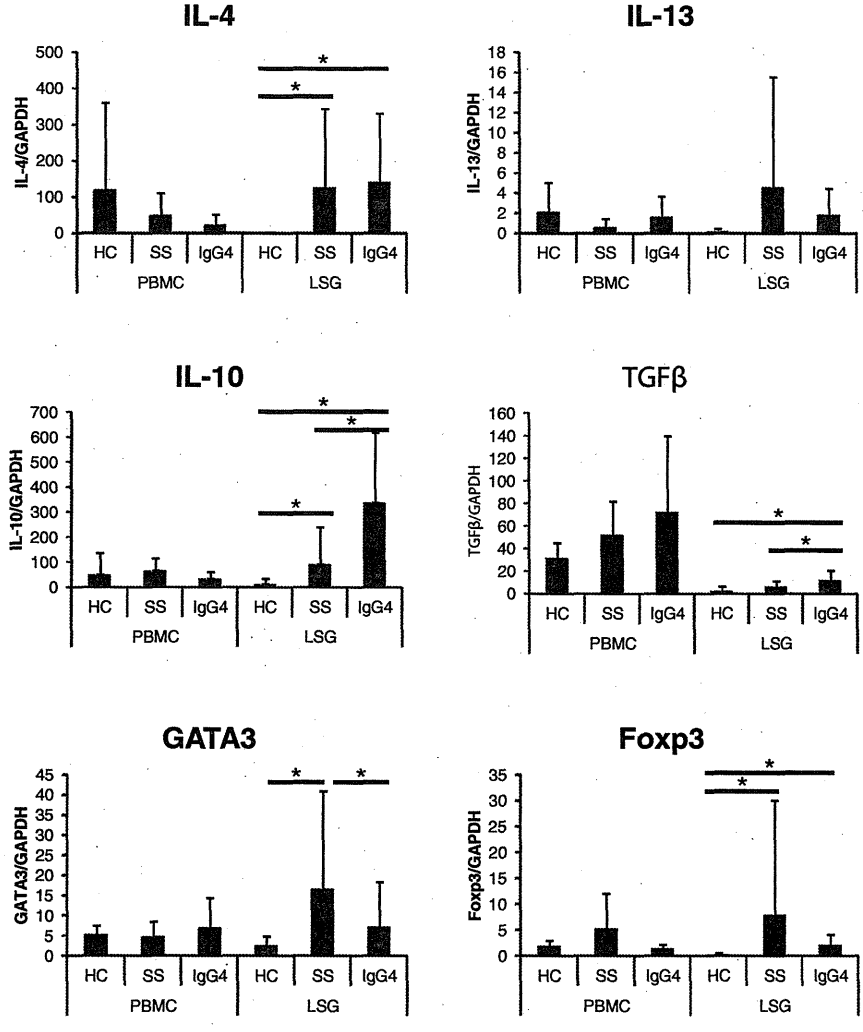


**Figure 2 The mRNA expression levels of IgG4-specific class switch-related molecules in PBMCs and LSGs.** The displayed mRNA expression levels are relative to the mRNA level of GAPDH, representing the internal control. Data are expressed as mean ± SD. *$P < 0.05$, Mann-Whitney *U* test. PBMCs, peripheral blood mononuclear cells; LSGs, labial salivary glands; HC, healthy control; SS, Sjögren syndrome; IgG4, IgG4-RD.

sorted from PBMCs, among the three groups (data not shown).

### The mRNA expression levels of IgG4-nonspecific class switch-related molecules in PBMCs, CD3-positive T cells, and CD20-positive B cells in PBMCs and LSGs

Figure 3 displays the mRNA expression levels of IgG4-nonspecific class switch-related molecules in PBMCs and LSGs. The mRNA expression levels of CD40 and CD154 were significantly lower in PBMCs of IgG4-RD than in SS ($P < 0.05$, each; Mann-Whitney *U* test). The expression of BAFF was significantly higher in LSGs of IgG4-RD than in the control ($P < 0.05$; Mann-Whitney *U* test). The expression of APRIL was significantly lower in PBMCs of IgG4-RD than in the control ($P < 0.05$; Mann-Whitney *U* test). The expression of AID was significantly higher in LSGs of IgG4-RD than in SS and the control ($P < 0.05$, each; Mann-Whitney *U* test).

Figure 4 shows the mRNA expression levels of IgG4-nonspecific class switch-related molecules in CD3-positive T cells and CD20-positive B cells sorted from PBMCs. In contrast to PBMCs, the expressions of CD40 in CD20-positive B cells and that of CD154 in CD3-positive T cells were comparable in the three groups. Moreover, no significant difference occurred in the expression of APRIL in CD3-positive T cells and CD20-positive B cells sorted from PBMCs, among the three groups. The expression of AID in CD20-positive B cells

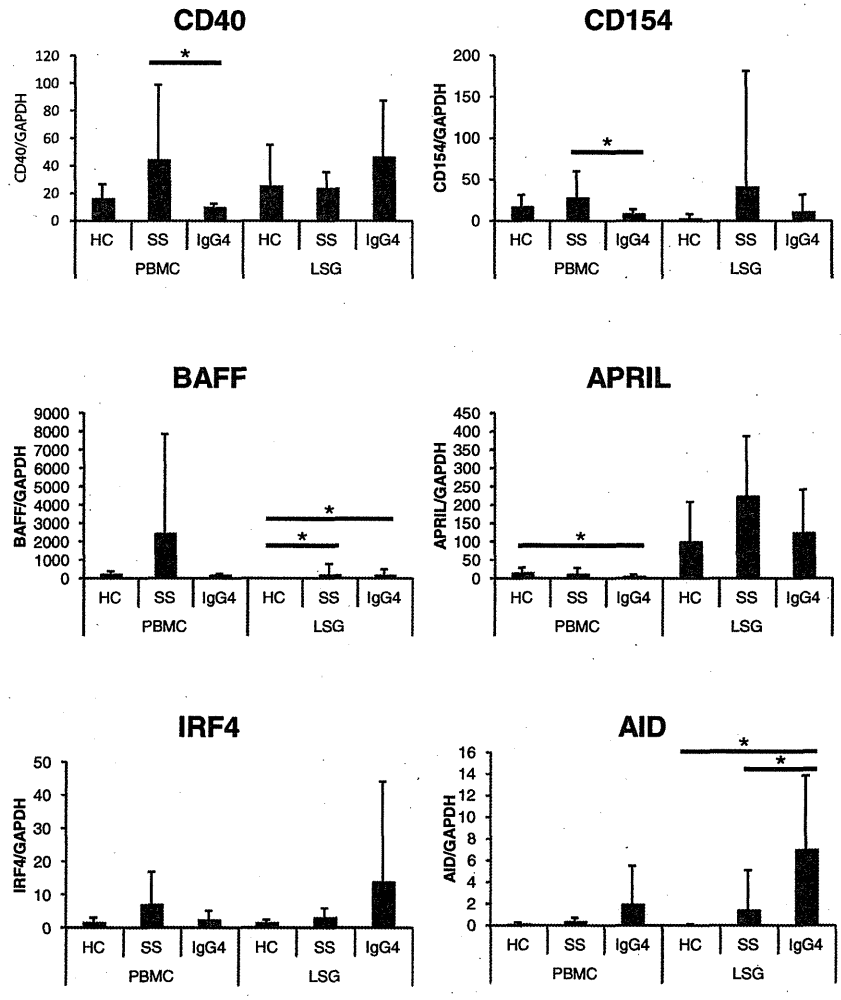


**Figure 3 The mRNA expression levels of IgG4-nonspecific class switch-related molecules in PBMCs and LSGs.** The displayed mRNA expression levels are relative to the mRNA level of GAPDH, representing the internal control. Data are expressed as mean ± SD. *$P < 0.05$, Mann-Whitney *U*-test. PBMCs, peripheral blood mononuclear cells; LSGs, labial salivary glands; HC, healthy control; SS, Sjögren syndrome; IgG4, IgG4-RD.

from IgG4-RD was higher than others (no statistically significant difference).

## Discussion

The clinical and pathologic features of patients with IgG4-RD participating in this study (such as low frequencies of anti SS-A antibodies and anti SS-B antibodies, high serum IgG4 levels, high IgG4/IgG in LSGs, and low CH50 levels) accord with previous reports [1].

We revealed the mRNA expression levels of IgG4-specific and nonspecific class switch-related molecules in both PBMCs and LSGs of IgG4-RD, and then, these levels were compared with those measured in patients with SS and controls. We focused on the molecules with different expression levels in IgG4-RD than in SS and control, with the assumption that these molecules could be IgG4-RD-specific pathogenic factors.

Among IgG4-specific class switch-related molecules, the expression levels of Treg cytokines (IL-10 and TGF-β) in LSGs of IgG4-RD were significantly higher than in SS and the control, in agreement with previous reports [4,5]. We assume that these cytokines might be produced by Treg cells in LSGs of IgG4-RD. According to this speculation, the mRNA expression level of Foxp3, which is a master transcriptional factor for Treg cells, was higher in LSGs of IgG4-RD than in the control. We also showed that the expression of GATA3 was significantly lower in LSGs of IgG4-RD than in SS. It is reported that in salivary glands of SS, Th2 cells were detected as well as Th1 cells, and could

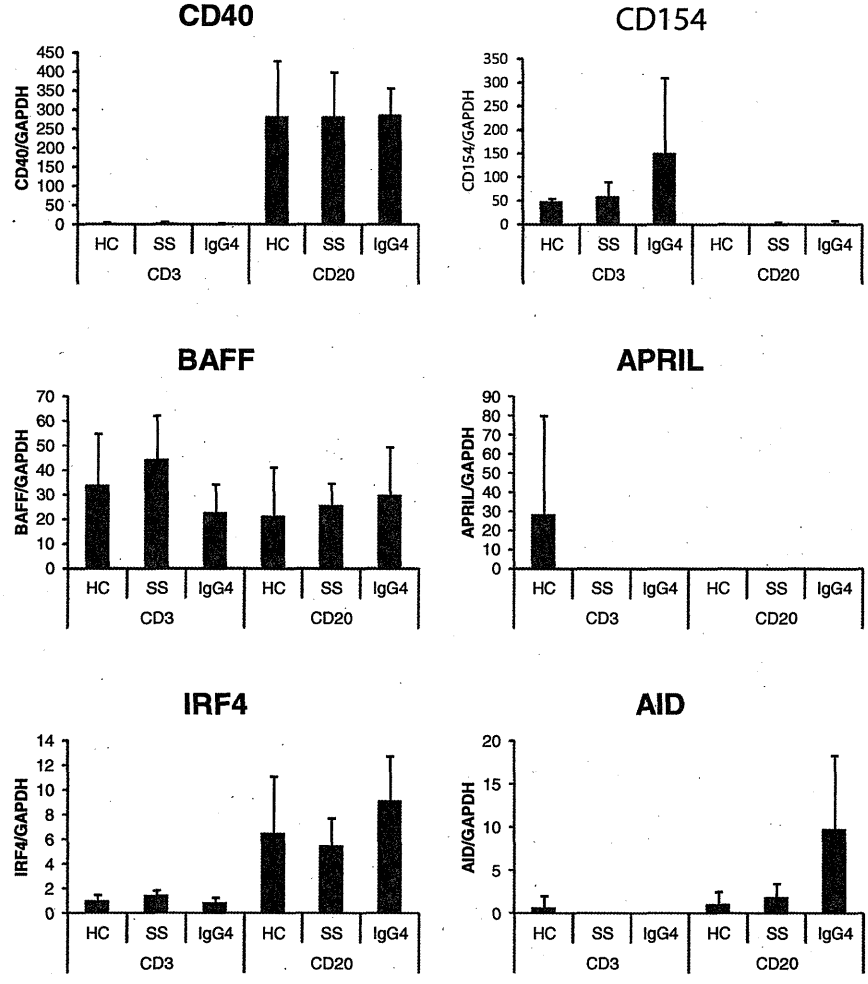


**Figure 4 The mRNA expression levels of IgG4-nonspecific class switch-related molecules in CD3-positive T cells and CD20-positive B cells sorted from PBMCs.** The displayed mRNA expression levels are relative to the mRNA level of GAPDH, representing the internal control. Data are expressed as mean ± SD. *$P < 0.05$; Mann-Whitney's *U* test. CD3, CD3-positive T cells sorted from PBMCs; CD20, CD20-positive B cells sorted from PBMCs; HC, healthy control; SS, Sjögren syndrome; IgG4, IgG4-RD.

contribute to activation of B cells through production of IL-4 [17]. Therefore, the lower mRNA expression of GATA3, a master transcriptional factor for Th2 cells, in IgG4-RD than in SS might be upregulation in SS but not downregulation in IgG4-RD. In SS, impaired Treg response or imbalance between a Treg response and a proinflammatory response might cause upregulation of Th1 and Th2 response that contributed to the pathophysiology of SS. Conversely, in IgG4-RD, upregulation of the Treg response itself could contribute to pathogenesis. Interestingly, it was previously reported that IL-10 enhanced IgG4 production from IL-4-stimulated PBMCs *in vitro* [9]. Therefore, in LSGs of IgG4-RD, IL-10 might induce IgG4-specific class-switch recombination, and TGF-β might cause tissue fibrosis [5,11]. Thus, Treg cytokines (IL-10 and TGF-β) might play important roles in IgG4-specific class-switch recombination and fibrosis, which are characteristic features of IgG4-RD.

Among IgG4-nonspecific class switch-related molecules, the expression of AID was significantly higher in LSGs of IgG4-RD than in SS and the control. The roles of IgG4-nonspecific class switch-related molecules such as AID in the pathogenesis of IgG4-RD have not been reported previously. The present study showed that the expression level of AID was different in IgG4-RD than in SS and the control. AID is essential for nonspecific immunoglobulin class-switch recombination (from IgM to IgG1, IgG2, IgG3, IgG4, IgA, and IgE) [12-14]; thus, upregulation of AID could also contribute to upregulation of IgG4-specific

class-switch recombination along with IL-10 in LSGs of IgG4-RD.

We showed that in SS, the population of CD20-positive B cells in PBMCs was much more than IgG4-RD and the control (statistically not significant). Therefore, CD40 and CD154 mRNAs in PBMCs of SS were highly expressed compared with that in IgG4-RD. These findings might be due to systemic B-cell activation in SS patients instead of local B-cell activation in IgG4-RD. Moreover, in CD3-positive T cells and CD20-positive B cells sorted from PBMCs, we found no IgG4-specific, -nonspecific, class switch-related molecules with different expression levels in IgG4-RD than in SS and controls.

These observations on the expression levels of AID and Treg cytokines suggest that IgG4 class-switch recombination in IgG4-RD was upregulated mainly in the tissues of the affected organs. However, the mechanism of upregulation of Treg cytokines in IgG4-RD is unknown. Treg response itself primarily regulates the immune response and inflammation [17]; therefore, increased Treg cytokines could be a nonspecific response to dampen the inflammation, which could increase the IgG4 class switch in the tissues.

## Conclusion

This study showed different expression levels of IgG4 class switch-related molecules in LSGs than in PBMCs of IgG4-RD. In LSGs of IgG4-RD, increased Treg cytokines (IL-10 and TGF-β) might play pathogenic roles in IgG4-specific class-switch recombination and fibrosis. AID was also increased in LSGs of IgG4-RD and could contribute to upregulation of IgG4-specific class-switch recombination along with IL-10 in LSGs. Thus, overexpression of IL-10, TGF-β, and AID in LSGs might play important pathogenic roles in IgG4-RD. IgG4 class-switch recombination seemed to be mainly upregulated in affected organs.

### Abbreviations

AID: activation-induced cytidine deaminase; APRIL: a proliferation-inducing ligand; BAFF: B cell-activating factor belonging to the tumor necrosis factor family; IgG4-RD: IgG4-related disease; IRF4: interferon regulatory factor 4; LSG: labial salivary gland; PBMC: peripheral blood mononuclear cell; SS: Sjögren syndrome.

### Acknowledgements

This work was supported by the Research Program for Intractable Diseases, Health and Labor Sciences Research Grants from the Ministry of Health, Labor and Welfare, Japan.

### Author details

[1]Department of Internal Medicine, Faculty of Medicine, University of Tsukuba, 1-1-1 Tennodai, Tsukuba, 305-8575, Japan. [2]Faculty of Dental Science, Kyushu University, 3-1-1 Maidashi, Fukuoka, 812-8582, Japan.

### Authors' contributions

All authors have read and approved the manuscript for publication. Each author took part in the design of the study, contributed to data collections, participated in writing the manuscript, and all agree to accept equal responsibility for accuracy of the contents of this article.

### Competing interests

The authors declare that they have no competing interests.

**Received: 1 April 2012 Accepted: 23 July 2012 Published: 23 July 2012**

### References

1. Umehara H, Okazaki K, Masaki Y, Kawano M, Yamamoto M, Saeki T, Matsui S, Sumida T, Mimori T, Tanaka Y, Tsubota K, Yoshino T, Kawa S, Suzuki R, Takegami T, Tomosugi N, Kurose N, Ishigaki Y, Azumi A, Kojima M, Nakamura S, Inoue D: **A novel clinical entity, IgG4-related disease (IgG4RD): general concept and details.** *Mod Rheumatol* 2012, **22**:1-14.
2. John HS, Yoh Z, Vikram D: **IgG4-related disease.** *N Engl J Med* 2012, **366**:539-551.
3. Zen Y, Fujii T, Harada K, Kawano M, Yamada K, Takahira M, Nakanuma Y: **Th2 and regulatory immune reaction are increased in immunoglobin G4-related sclerosing pancreatitis and cholangitis.** *Hepatology* 2007, **45**:1538-1546.
4. Miyake K, Moriyama M, Aizawa K, Nagano S, Inoue Y, Sadanaga A, Nakashima H, Nakamura S: **Peripheral CD4+ T cells showing a Th2 phonotype in a patient with Mikulicz's disease associated with lymphadenopathy and pleural effusion.** *Mod Rheumatol* 2008, **18**:86-90.
5. Tanaka A, Moriyama M, Nakashima H, Miyake K, Hayashida JN, Maehara T, Shinozaki S, Kubo Y, Nakamura S: **Th2 and regulatory immune reactions contribute to IgG4 production and the initiation of Mikulicz's disease.** *Arthritis Rheum* 2012, **64**:254-263.
6. Nakashima H, Miyake K, Moriyama M, Tanaka A, Watanabe M, Abe Y, Sato H, Nakamura S, Saito T: **An amplification of IL-10 and TGF-beta in patients with IgG4-related tubulointerstitial nephritis.** *Clin Nephrol* 2010, **73**:385-391.
7. Akitake R, Watanabe T, Zaima C, Uza N, Ida H, Tada S, Nishida N, Chiba T: **Possible involvement of T helper type 2 responses to Toll-like receptor ligands in IgG4-related sclerosing disease.** *Gut* 2010, **59**:542-545.
8. Miyoshi H, Uchida K, Taniguchi T, Yazumi S, Matsushita M, Takaoka M, Okazaki K: **Circulating naïve and $CD4^+CD25$-high regulatory T cells in patients with autoimmune pancreatitis.** *Pancreas* 2008, **36**:133-140.
9. Jeannin P, Lecoanet S, Delneste Y, Gauchat JF, Bonnefoy JY: **IgE versus IgG4 production can be differentially regulated by IL-10.** *J Immunol* 1998, **160**:3555-3561.
10. Reefer AJ, Carneiro RM, Custis NJ, Platts-Mills TA, Sung SS, Hammer J, Woodfolk JA: **A role for IL-10-mediated HLA-DR7-restricted T cell dependent events in development of the modified Th2 response to cat allergen.** *J Immunol* 2004, **172**:2763-2772.
11. Biernacka A, Dobaczewski M, Frangogiannis NG: **TGF-β signaling in fibrosis.** *Growth Factors* 2011, **29**:196-202.
12. Clifford MS, Kenneth BM, Piotr Z: **The immunoglobulin class switch: beyond "Accessibility".** *Immunity* 1997, **6**:217-223.
13. Avery DT, Bryant VL, Ma CS, Malefyt RW, Tangye SG: **IL-21-induced isotype switching to IgG and IgA by human naïve B cells is differentially regulated by IL-4.** *J Immunol* 2008, **181**:1767-1779.
14. Arthur LS, NC Tolga Emre, Paul BR, Louis MS: **IRF4: Immunity. Malignancy! Therapy?** *Clin Cancer Res* 2009, **15**:2954-2961.
15. Umehara H, Okazaki K, Masaki Y, Kawano M, Yamamoto M, Saeki T, Matsui S, Yoshino T, Nakamura S, Kawa S, Hamano H, Kamisawa T, Shimosegawa T, Shimatsu A, Nakamura S, Ito T, Notohara K, Sumida T, Tanaka Y, Mimori T, Chiba T, Mishima M, Hibi T, Tsubouchi H, Inui K, Ohara H: **Comprehensive diagnostic criteria for IgG4-related disease (IgG4-RD), 2011.** *Mod Rheumatol* 2012, **22**:21-30.
16. Fujibayashi T, Sugai S, Miyasaka N, Hayashi Y, Tsubota K: **Revised Japanese criteria for Sjögren's syndrome (1999): availability and validity.** *Mod Rheumatol* 2004, **14**:425-434.
17. Gikas EK, Niki MM, Sharon MM: **T lymphocytes in Sjögren's syndrome: contributors to and regulators of pathophysiology.** *Clin Rev Allerg Immunol* 2007, **32**:252-264.

**doi:10.1186/ar3924**
**Cite this article as:** Tsuboi *et al.*: **Analysis of IgG4 class switch-related molecules in IgG4-related disease.** *Arthritis Research & Therapy* 2012 **14**: R171.

ARTHRITIS & RHEUMATISM
Vol. 64, No. 12, December 2012, pp 3877–3885
DOI 10.1002/art.34666


# Murine Tumor Necrosis Factor α–Induced Adipose-Related Protein (Tumor Necrosis Factor α–Induced Protein 9) Deficiency Leads to Arthritis via Interleukin-6 Overproduction With Enhanced NF-κB, STAT-3 Signaling, and Dysregulated Apoptosis of Macrophages

Asuka Inoue,[1] Isao Matsumoto,[1] Yoko Tanaka,[1] Naoto Umeda,[1] Yuki Tanaka,[1] Masahiko Mihara,[2] Satoru Takahashi,[1] and Takayuki Sumida[1]

***Objective.*** **To elucidate the role of tumor necrosis factor α–induced adipose-related protein (TIARP; or tumor necrosis factor α–induced protein 9 [TNFAIP-9]) in the development and pathogenesis of arthritis.**

***Methods.*** **We generated TIARP-deficient ($TIARP^{-/-}$) mice and investigated several organs in aged mice. Peritoneal macrophages were collected and cultured with lipopolysaccharide (LPS) and TNFα, and then the production of cytokines and subsequent NF-κB signal transduction were analyzed. We also examined the susceptibility of young $TIARP^{-/-}$ mice to collagen-induced arthritis (CIA). Draining lymph nodes and splenocytes were isolated and cultured, and serum levels of anti–type II collagen (anti-CII) antibodies, interleukin-6 (IL-6), and TNFα on day 60 were measured. We further investigated the effects of anti–IL-6 receptor monoclonal antibody (mAb) on the development of arthritis in $TIARP^{-/-}$ mice. IL-6/STAT-3 signaling was also analyzed using $TIARP^{-/-}$ macrophages.**

***Results.*** **$TIARP^{-/-}$ mice developed spontaneous enthesitis and synovitis, had high serum levels of IL-6, had increased CD11b+ cell counts in the spleen, and showed enhanced LPS- and TNFα-induced IL-6 expression in macrophages. Sustained degradation of IκBα with dysregulated apoptosis was also noted in $TIARP^{-/-}$ macrophages. CIA was clearly exacerbated in $TIARP^{-/-}$ mice, accompanied by marked neutrophil and macrophage infiltration in joints. The levels of anti-CII antibodies in serum were unchanged, whereas autoreactive Th1 cell and Th17 cell responses were higher in $TIARP^{-/-}$ mice. Treatment with anti–IL-6 receptor mAb prevented the development of CIA in $TIARP^{-/-}$ mice, and $TIARP^{-/-}$ macrophages showed increased IL-6–induced STAT-3 phosphorylation.**

***Conclusion.*** **These findings suggest that TIARP acts as a negative regulator of arthritis by suppressing IL-6 production, its signaling and TNFα-induced NF-κB signaling, resulting in enhanced apoptosis in macrophages.**

The prognosis in patients with rheumatoid arthritis (RA) has improved significantly with the recent availability of biologic agents that target tumor necrosis factor α (TNFα) and interleukin-6 (IL-6) (1,2). However, the exact mechanisms of action of these agents remain largely unknown. Glucose-6-phosphate isomerase (GPI) was first identified as an arthritogenic target in K/BxN mice (3), and GPI immunization of DBA/1 mice was shown to lead to arthritis (GPI-induced arthritis) (4). Studies in GPI-induced arthritis showed clear therapeutic benefits of treatment with TNFα and IL-6 antagonists (5,6), suggesting its suitability for analyzing the mechanisms of action of these agents in RA.

Using GeneChip analysis, we previously demon-

Supported in part by a grant from the Japanese Ministry of Science and Culture to Drs. Matsumoto and Sumida.

[1]Asuka Inoue, PhD, Isao Matsumoto, MD, PhD, Yoko Tanaka, PhD, Naoto Umeda, MD, Yuki Tanaka, MS, Satoru Takahashi, MD, PhD, Takayuki Sumida, MD, PhD: Graduate School of Comprehensive Human Sciences, University of Tsukuba, Tsukuba, Japan; [2]Masahiko Mihara, PhD: Chugai Pharmaceutical Company, Gotemba, Japan.

Dr. Matsumoto has received a research grant from Bristol-Myers Squibb.

Address correspondence to Isao Matsumoto, MD, PhD, Division of Clinical Immunology, Doctoral Program in Clinical Science, Graduate School of Comprehensive Human Sciences, University of Tsukuba, 1-1-1 Tennodai, Tsukuba 305-8575, Japan. E-mail: ismatsu@md.tsukuba.ac.jp.

Submitted for publication March 1, 2012; accepted in revised form August 2, 2012.

strated the up-regulation of TNFα-induced adipose-related protein (TIARP) in GPI-induced arthritis (7), as well as in CD11b+ splenocytes and joints of mice. Human TIARP counterparts, such as 6-transmembrane epithelial antigen of prostate 4 (STEAP-4), were also found to be highly expressed in peripheral blood monocytes, neutrophils, and synovial CD68+ cells from patients with RA (7,8). However, the role of TIARP in the pathogenesis of autoimmune arthritis remains to be confirmed.

In this study, we found that TIARP-deficient ($TIARP^{-/-}$) mice develop spontaneous enthesitis and synovitis, with high numbers of macrophages and elevated IL-6 expression. $TIARP^{-/-}$ macrophages showed enhanced NF-κB signaling, with dysregulated TNFα-induced apoptosis, and showed increased IL-6–induced STAT-3 phosphorylation. Moreover, the development of collagen-induced arthritis (CIA) was markedly exacerbated in $TIARP^{-/-}$ mice, suggesting that TIARP may provide new insights into the pathogenesis of arthritis as a negative regulator.

## MATERIALS AND METHODS

**Mice.** The $TIARP^{-/-}$ mouse line was generated by homologous recombination in embryonic stem cells from mice of the C57BL/6 (B6) background. A conditional targeting vector for the TIARP gene was designed to delete exon 2, with a DNA fragment containing a loxP-flanked neomycin resistance gene and herpes simplex virus thymidine kinase gene (illustration available upon request from the corresponding author). All mice were maintained under specific pathogen–free conditions in an environmentally controlled clean room at the University of Tsukuba. All animal experiments were approved by the institutional committee and were conducted in accordance with the institutional ethics guidelines.

**Histopathologic examination.** When the mice were 12 months of age, we removed the primary organs and tissues, including the ankle joints, lungs, salivary glands, white adipose tissue, liver, thymus, spleen, inguinal lymph nodes, stomach, small intestine, large intestine, kidneys, and reproductive organs, for histopathologic examination. Tissues were fixed in neutralized 10% formalin, and the joints of the right hind paw were decalcified in 10% formic acid and embedded in paraffin. We stained 4-mm serial sections with hematoxylin and eosin or toluidine blue and scored the tissues for histologic changes. Sections were graded on a scale of 0–5, where 0 = normal and 5 = severe. One point was given for the presence of each of the following features of enthesitis: inflammatory cell infiltration, entheseal fibroblast-like cell proliferation, cartilage formation, bone formation, and ankylosis. The same system was used to grade synovitis, with 1 point given for each of the following features: inflammatory cell infiltration, synovial hyperplasia, pannus formation, cartilage degradation, and bone degradation.

For immunohistochemical staining, the sections were incubated overnight at 4°C with rat anti–Gr-1 or anti-F4/80. The signals were detected with Alexa 488–conjugated anti-rat IgG. Nuclei were counterstained with DAPI. The sections were examined under fluorescence microscopy (Keyence).

**Flow cytometric analysis.** For flow cytometry, cells were stained with fluorescein isothiocyanate (FITC)–, phycoerythrin-, PerCP-, or allophycocyanin-conjugated monoclonal antibodies (mAb). Rat mAb to mouse CD3, CD4, CD8, CD11b, Gr-1, F4/80, CD11c, IL-17, and interferon-γ (IFNγ) were purchased from BioLegend, and rat mAb to mouse FoxP3 was purchased from eBioscience. Apoptosis was detected by staining with propidium iodide and FITC-conjugated annexin V (BioLegend). We performed cell surface staining according to standard techniques. Stained cells were identified with a FACSCalibur cytometer (Becton Dickinson) using FlowJo software (Tree Star).

**Real-time quantitative polymerase chain reaction (PCR) analysis.** We isolated total RNA from splenocytes and ankle joints by the Isogen (Nippon Gene) extraction method according to the instructions provided by the manufacturer. We performed real-time quantitative PCR as described previously (7) using a TaqMan gene expression assay (Applied Biosystems) and the following probes: TIARP (Mm00475402_m1), TNFα (Mm00443258_m1), IL-6 (Mm00446190_m1), CXCL2 (Mm00436450_m1), matrix metalloproteinase 3 (MMP-3) (Mm00440295_m1), RANKL (Mm00441906_m1), and GAPDH (Mm99999915_g1). Real-time quantitative PCR was carried out using an ABI 7500 analyzer (Applied Biosystems). Analysis of post-PCR melting curves confirmed the specificity of the single-target amplification. We determined the expression of each gene relative to GAPDH.

**Thioglycolate-elicited macrophages.** Mice were injected intraperitoneally with 2 ml of 3% thioglycolate. After 3 days, mice were euthanized and peritoneal macrophages were collected by phosphate buffered saline (PBS) lavage. Cells were incubated for the indicated durations in the presence or absence of 100 ng/ml of TNFα, 100 ng/ml of lipopolysaccharide (LPS), or 10 ng/ml of IL-6.

**Immunoblotting.** Cells were lysed in 0.5% Nonidet P40, 5 m*M* $MgCl_2$, 50 m*M* Tris HCl (pH 7.4), and 2 m*M* phenylmethylsulfonyl fluoride. Equal amounts of protein were subjected to immunoblotting using antibodies to IκBα, phospho-STAT-3, STAT-3, and suppressor of cytokine signaling 3 (SOCS-3), as well as phospho-ERK-1/2, ERK-1/2, caspase 3, cleaved caspase 3 antibodies (Cell Signaling Technology), and anti-actin antibodies (Bio-Rad). Densitometric analysis was carried out using an ImageQuant LAS 4000 densitometer (GE Healthcare).

**Collagen-induced arthritis.** CIA was induced in mice of the B6 background. We immunized 8–12-week-old mice intradermally at several sites at the base of the tail with 100 μl of 200 μg chicken type II collagen (CII; Sigma) emulsified in Freund's incomplete adjuvant (Difco) and containing 5 mg/ml of heat-killed *Mycobacterium tuberculosis* (H37Ra; Difco). According to the usual immunization schedule, mice were rechallenged with CII and Freund's complete adjuvant on day 21 after the primary immunization. Arthritis was assessed every other day by examining each joint for swelling and redness. Arthritis severity was graded on a scale of 0–3 in each paw. The clinical score for each mouse was the sum of the scores for the 4 paws (maximum score 12).

**Enzyme-linked immunosorbent assay (ELISA).** Single-cell suspensions were prepared from the spleens and lymph nodes of wild-type (WT) and $TIARP^{-/-}$ mice. Cells were

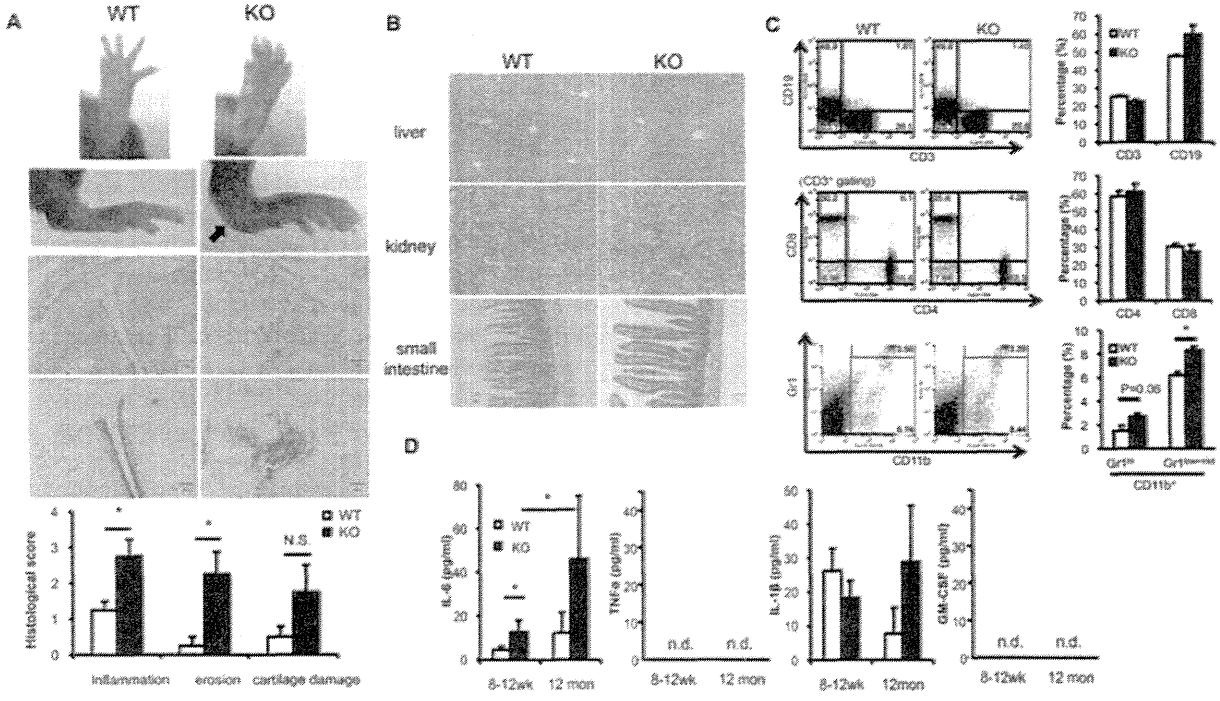


**Figure 1.** Development of arthritis in aged tumor necrosis factor $\alpha$–induced adipose-related protein (TIARP)–knockout (KO) mice, with increased numbers of macrophages and overproduction of interleukin-6 (IL-6) as compared to wild-type (WT) mice. **A,** Macroscopic (top) and microscopic (middle) appearance of the ankle joints of 12-month-old WT and TIARP$^{-/-}$ mice, along with histology scores (bottom). **Arrow** in the ankle joint photograph indicates inflammatory changes. Photomicrographs of hematoxylin and eosin (H&E)–stained (top) and toluidine blue–stained (bottom) sections of the ankle joints demonstrate the histopathologic changes. Original magnification × 20. Histology scores for inflammation, erosion, and cartilage damage were higher in the TIARP$^{-/-}$ mice. Values are the mean ± SEM of 2 independent experiments (n = 5 mice per group per experiment). * = $P < 0.05$, by Student's *t*-test. NS = not significant. **B,** Histologic assessment of H&E-stained sections of liver, kidney, and small intestine from WT and TIARP$^{-/-}$ mice. Original magnification × 20. **C,** Flow cytometry of splenocytes from 12-month-old WT and TIARP$^{-/-}$ mice (left) and percentages of the indicated cell subsets (right). Cells were stained with a combination of antibodies and analyzed as described in Materials and Methods. Values in each compartment are the percentages of cells. The percentages of splenic CD11b+Gr-1$^{high}$ cells (neutrophils) and CD11b+Gr-1$^{low/intermediate}$ cells (macrophages) were determined. Values are the mean ± SEM of 2 independent experiments (n = 5 mice per group per experiment). * = $P < 0.05$, by Student's *t*-test. **D,** Serum concentrations of IL-6, tumor necrosis factor $\alpha$ (TNF$\alpha$), IL-1$\beta$, and granulocyte–macrophage colony-stimulating factor (GM-CSF) in 8–12-week-old and 12-month-old mice. Values are the mean ± SEM of 2 independent experiments (n = 5 mice per group per experiment). * = $P < 0.05$, by Student's *t*-test. ND = not detected.

cultured for 72 hours at 37°C in an atmosphere containing 5% $CO_2$, and supernatants were collected. Levels of IL-6 and TNF$\alpha$ in the cell culture supernatants were measured using ELISA kits (R&D Systems). Serum samples were collected on days 30 and 60 from arthritic WT and TIARP$^{-/-}$ mice, and serum levels of TNF$\alpha$, IL-6, IL-1$\beta$, and granulocyte–macrophage colony-stimulating factor (GM-CSF) were measured with ELISA kits (R&D Systems). Serum levels of anti-CII antibodies were also analyzed for CII-specific IgG antibodies by ELISA. All serum samples were diluted 1:3,000 in PBS prior to ELISA.

**Treatment of arthritis with anticytokine antibodies.** For IL-6 neutralization, mice were injected intraperitoneally with 2 mg of MR16-1 (a rat IgG1 mAb against murine IL-6 receptor [IL-6R]) or control IgG (purified from the serum of nonimmunized rats) on day 21 after induction of CIA. MR16-1 was a gift from Chugai Pharmaceutical, and control IgG was purchased from Jackson ImmunoResearch. To neutralize TNF$\alpha$, mice were injected intraperitoneally with 100 $\mu$g of neutralizing antibody or isotype control on day 21. Anti-TNF$\alpha$ mAb MP6-XT3 (IgG1, rat) and IgG1 isotype control (rat) were purchased from eBioscience.

**Statistical analysis.** In the CIA experiments, disease incidence was evaluated with the chi-square test and the severity score by the Mann-Whitney U test. Student's *t*-test was used for the evaluation of all other results. *P* values less than 0.05 were considered significant.

## RESULTS

**Spontaneous development of destructive arthritis, with increased numbers of macrophages and high serum levels of IL-6, in TIARP-deficient mice.** TIARP$^{-/-}$ mice were generated to further investigate

**Table 1.** Abnormal clinical and histologic features in aged (12-month-old) male TIARP$^{-/-}$ mice as compared with their wild-type littermates

| Characteristic | Wild-type mice (n = 13) | Knockout mice (n = 13) |
|---|---|---|
| Clinical features | | |
| Incidence of arthritis, no. (%) | 0 (0.0) | 10 (76.9)* |
| Mean ± SEM clinical score | 0.00 ± 0.00 | 2.25 ± 0.62* |
| Histologic score | | |
| Inflammation, mean ± SEM | 1.25 ± 0.25 | 2.75 ± 0.48† |
| Erosions, mean ± SEM | 0.25 ± 0.25 | 2.25 ± 0.63† |
| Cartilage damage, mean ± SEM | 0.50 ± 0.29 | 1.75 ± 0.75† |

* $P < 0.005$.
† $P < 0.05$.

the function of TIARP in arthritis. To do this, we used homologous recombination in embryonic stem cells derived from B6 mice to produce a line of mice carrying a defective TIARP gene. In the homozygous state, these mice carry a mutant allele with exon 2 deleted (data available upon request from the corresponding author). The expression of the mature TIARP gene and protein in splenocytes, peritoneal macrophages, and synoviocytes (data not shown) could not be detected by real-time quantitative PCR and Western blotting.

We then tested whether deletion of the TIARP gene could directly induce organ autoimmunity. We found that 76.9% of the deficient mice developed joint abnormalities by 12 months of age (Figure 1A and Table 1). Furthermore, marked enthesopathy and weak synovitis with joint destruction were observed in these TIARP$^{-/-}$ mice (Figure 1A). These findings were confirmed by histologic scoring of inflammation and erosion (Figure 1A). We also screened several other organs isolated from 20-week-old and 12-month-old mice. The murine white adipose tissues showed weak cell infiltration, confirming the findings of Wellen et al (9), although there was no significant cell infiltration or damage in the liver, kidney, or small intestine (Figure 1B) or in the white adipose tissue, large intestine, or other organs (data available upon request from the corresponding author).

Immune cell development and function in TIARP$^{-/-}$ mice were investigated next. The involvement of acquired immune cells in the spleen (Figure 1C) and in the thymus and mesenteric and inguinal lymph nodes (LNs) (data not shown) in TIARP$^{-/-}$ mice was almost comparable to WT mice. Because TIARP is highly expressed in CD11b+ cells during GPI-induced arthritis (7), we screened the spleens of TIARP$^{-/-}$ mice and found significantly high numbers of CD11b+

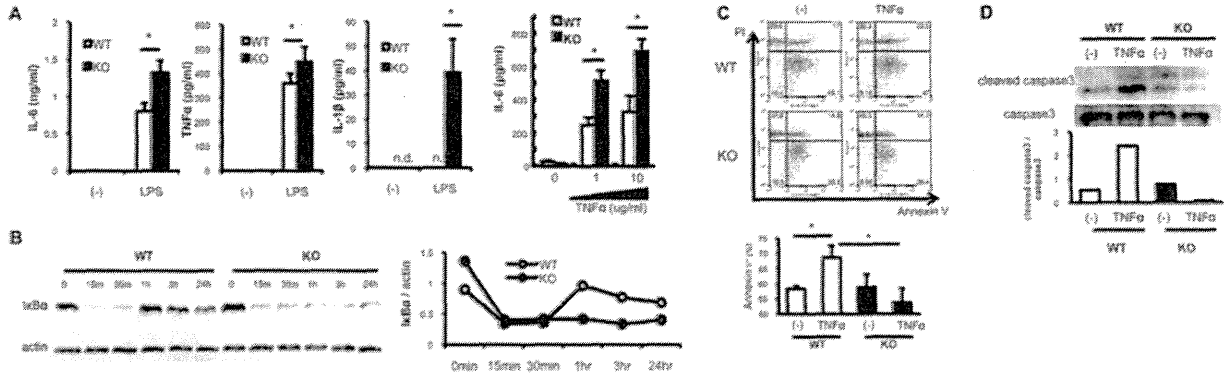


**Figure 2.** Enhanced responsiveness of macrophages from TIARP$^{-/-}$ mice to lipopolysaccharide (LPS) and TNFα. **A**, Levels of IL-6, TNFα, and IL-1β in culture supernatants, as determined by enzyme-linked immunosorbent assay. Thioglycolate-elicited macrophages from TIARP$^{-/-}$ and WT mice were cultured for 12 hours in the presence or absence of LPS or were cultured for 96 hours in the presence or absence of 1 μg/ml or 10 μg/ml of TNFα. Values are the mean ± SEM of 3 independent experiments (n = 5 mice per group per experiment). * = $P < 0.05$. **B**, Levels of IκBα in extracts of thioglycolate-elicited macrophages from TIARP$^{-/-}$ and WT mice, as determined by immunoblot analysis. Cells were incubated with 100 ng/ml of TNFα for the indicated times, and immunoblotting was performed, as shown at the left. Actin was used as a loading control. Results of densitometric quantification of IκBα levels are shown at the right. Values are the mean. **C**, Flow cytometry of apoptotic cell populations in macrophages left unstimulated or stimulated for 24 hours with TNFα, as detected by propidium iodide and annexin V staining. Percentages of annexin V+ cells are shown at the bottom. Values are the mean ± SEM of 2 independent experiments (n = 5 mice per group per experiment). * = $P < 0.05$. **D**, Analysis of caspase 3 and cleaved caspase 3 in macrophages. Thioglycolate-elicited macrophages were treated with 100 ng/ml of TNFα, and total cell lysates were immunoblotted with antibodies to cleaved caspase 3 (bands at 17 kd and 19 kd) or caspase 3, as shown at the top. Results of densitometric quantification of the ratio of cleaved caspase 3 to caspase 3 are shown at the bottom. Values are the mean. See Figure 1 for other definitions.

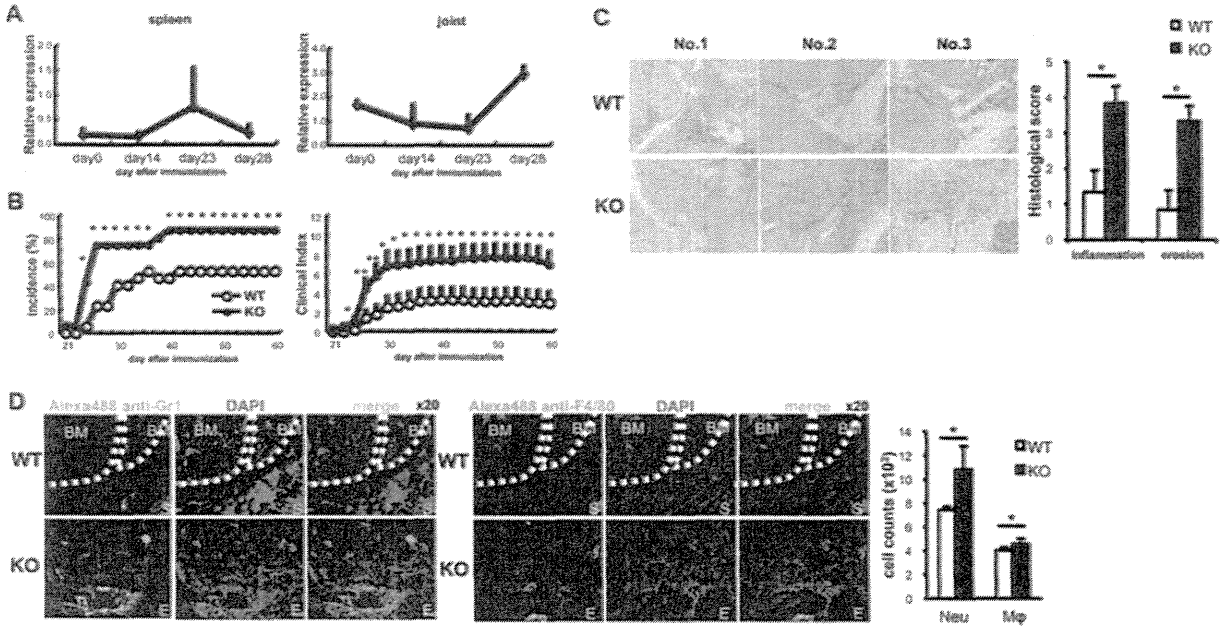

**Figure 3.** Exacerbation of collagen-induced arthritis (CIA), with marked infiltration of neutrophils and macrophages, in TIARP$^{-/-}$ mice. **A,** Expression of mRNA for TIARP in the spleen and joints obtained on the indicated days from TIARP$^{-/-}$ and WT mice with CIA. Values are the mean ± SEM of 3 independent experiments (n = 5 mice per group per experiment). **B,** Arthritis incidence and severity scores in TIARP$^{-/-}$ and WT mice with CIA. Values are the mean ± SEM of 3 independent experiments (n = 16–17 mice per group per experiment). * = $P < 0.05$. **C,** Histopathologic analysis of joint sections obtained on day 60 after immunization in 3 mice from each group. Original magnification × 20. Histopathology scores for inflammation and erosion are shown at the right. Values are the mean ± SEM of 2 independent experiments (n = 5 mice per group per experiment). * = $P < 0.05$. **D,** Immunofluorescence analysis of neutrophils and macrophages using anti–Gr-1 and anti-F4/80 monoclonal antibodies, respectively, in the bone marrow (BM), synovium (S), and exudate (E) of ankle joints obtained on day 60. Broken lines in the top panels of the photomicrographs indicate the surface of the articular cartilage. Original magnification × 20. Numbers of neutrophils and macrophages in the ankle joints as determined on day 60 are shown at the right. Values are the mean ± SEM of 2 independent experiments (n = 5 mice per group per experiment). * = $P < 0.05$. See Figure 1 for other definitions. Color figure can be viewed in the online issue, which is available at http://onlinelibrary.wiley.com/journal/10.1002/(ISSN)1529-0131.

Gr-1$^{low/intermediate}$ cells (confirmed by microscopy to be macrophages) (Figure 1C).

We next examined inflammatory cytokines in the TIARP$^{-/-}$ mice, since they are also key players in RA

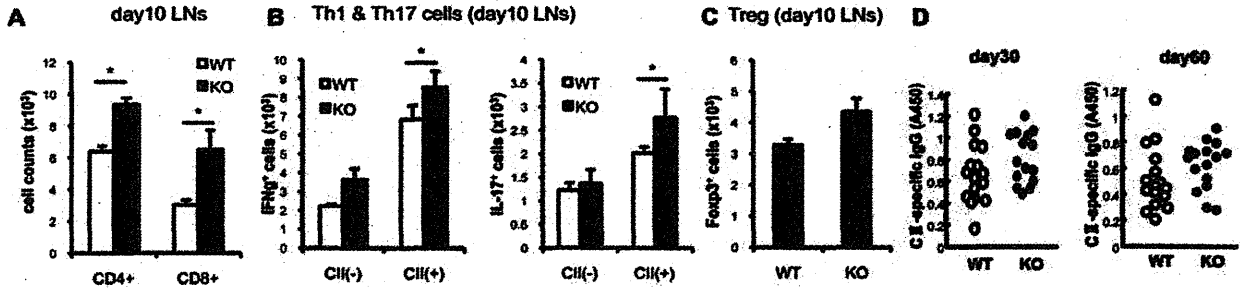

**Figure 4.** Enhanced type II collagen (CII)–specific Th1 cells and Th17 cells, with comparable amounts of anti-CII antibodies, in tumor necrosis factor α–induced adipose-related protein (TIARP)–knockout (KO) mice as compared to wild-type (WT) mice. **A,** Numbers of CD4+ and CD8+ cells in draining lymph nodes (LNs) obtained on day 10. Values are the mean ± SEM of 3 independent experiments (n = 5 mice per group per experiment). * = $P < 0.05$. **B** and **C,** Numbers of interferon-γ (IFNγ)–positive and interleukin-17 (IL-17)–positive cells (**B**) and numbers of FoxP3-positive Treg cells (**C**) in draining LNs obtained on day 10, as determined by flow cytometry, gating on CD3+CD4+ cells. Values are the mean ± SEM of 3 independent experiments (n = 5 mice per group per experiment). * = $P < 0.05$. **D,** Serum levels of CII-specific IgG in 16 WT mice and 17 TIARP$^{-/-}$ mice on day 30 and day 60 after immunization. Each symbol represents a single animal.

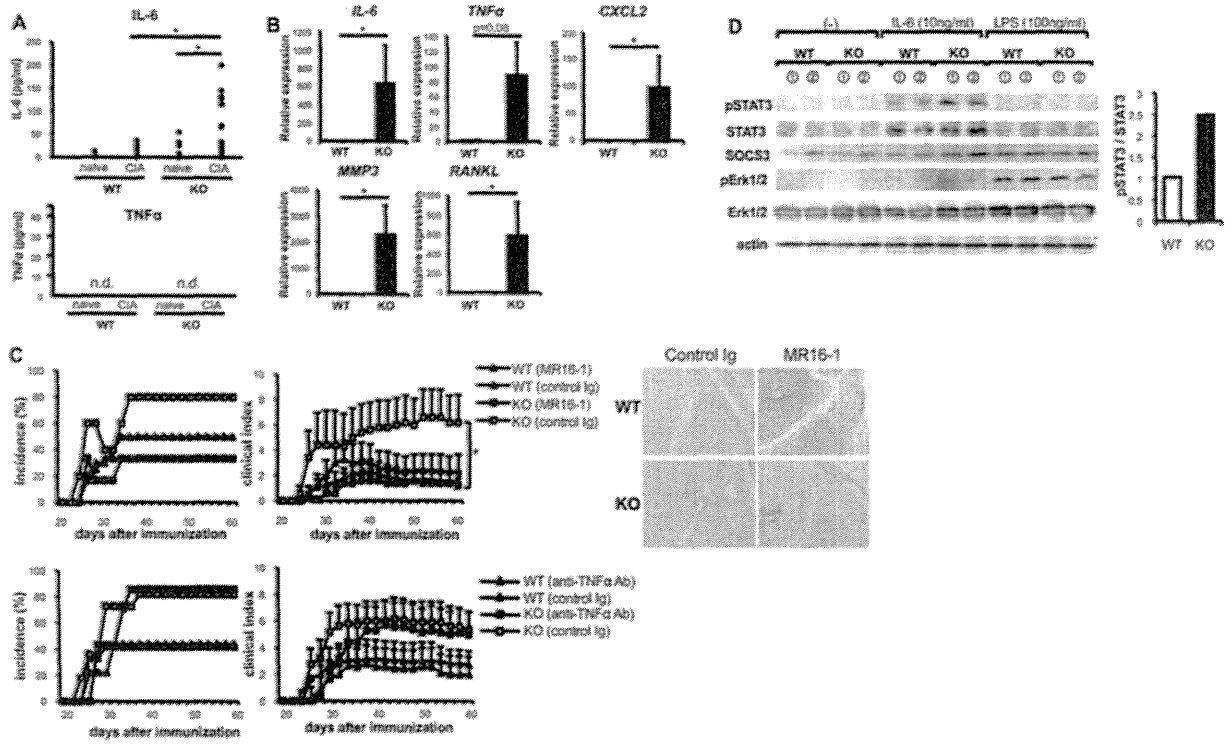


**Figure 5.** IL-6–triggered exacerbation of collagen-induced arthritis (CIA) in TIARP$^{-/-}$ mice. **A,** Serum levels of IL-6 (top) and TNFα (bottom) on day 0 and day 60 after immunization in naive mice (n = 10–12 mice per group per experiment) and mice with CIA (n = 16 WT mice and n = 17 TIARP$^{-/-}$ mice). Each symbol represents a single animal. **B,** Expression of IL-6, TNFα, CXCL2, matrix metalloproteinase 3 (MMP-3), and RANKL genes in ankle joints obtained on day 60, as determined by real-time polymerase chain reaction analysis. Values are the mean ± SEM of 2 independent experiments (n = 5 mice per group per experiment). * = $P < 0.05$. **C,** Arthritis incidence and severity scores on day 21 in mice treated with 2 mg of anti–IL-6 receptor (anti–IL-6R) monoclonal antibody (mAb; MR16-1) (top) or with 100 μg of anti-TNFα mAb (bottom). Values are the mean ± SEM. * = $P < 0.05$. Histopathologic analysis of ankle joint sections obtained on day 60 after immunization following treatment with control Ig or with MR16-1 mAb is shown at the right. Original magnification × 20. **D,** Levels of pSTAT-3, STAT-3, SOCS-3, pERK-1/2, and ERK-1/2 in cell lysates of thioglycolate-elicited macrophages from TIARP$^{-/-}$ and WT mice (n = 2 mice per group), as determined by immunoblot analysis. Cells were incubated for 1 hour in the absence or presence of 10 ng/ml of IL-6 or 100 ng/ml of lipopolysaccharide (LPS). Actin was used as a loading control. Results of densitometric quantification of the ratio of pSTAT-3 to STAT-3 are shown at the right. Values are the mean. See Figure 1 for other definitions. Color figure can be viewed in the online issue, which is available at http://onlinelibrary.wiley.com/journal/10.1002/(ISSN)1529-0131.

and are functionally linked to TIARP (10–12). Serum levels of IL-6 were higher in TIARP$^{-/-}$ mice than in WT mice irrespective of age, whereas no TNFα or GM-CSF was detected, and IL-1β levels were similar in WT and TIARP$^{-/-}$ mice (Figure 1D).

Taken together, these findings suggested that TIARP$^{-/-}$ mice develop spontaneous enthesopathy and synovitis, with elevated numbers of macrophages and elevated levels of IL-6, which suggest a pivotal role of macrophages.

**Increased response to LPS and TNFα, sustained degradation of IκBα, and resistance to TNFα-induced apoptosis in macrophages from TIARP$^{-/-}$ mice.** Next, we focused on CD11b+ cells, based on the dominant expression of TIARP in these cells in GPI-induced arthritis (7) and on the spontaneous aberrant accumulation of macrophages in TIARP$^{-/-}$ mice. Thioglycolate-activated peritoneal macrophages from TIARP$^{-/-}$ mice produced higher amounts of IL-6, TNFα, and IL-1β upon LPS stimulation (Figure 2A). Macrophages from TIARP$^{-/-}$ mice also produced higher amounts of IL-6 with TNFα stimulation (Figure 2A). Levels of IL-6Rα, TNF receptor type I (TNFRI), and TNFRII expression were similar in macrophages from TIARP$^{-/-}$ and WT mice (data not shown).

We then examined the role of TIARP in the NF-κB pathway and in apoptosis. Macrophages obtained from TIARP$^{-/-}$ mice and cultured with TNFα

showed sustained degradation of the NF-κB inhibitory molecule IκBα as compared to macrophages from WT mice (Figure 2B). Moreover, TNFα-induced apoptosis was increased in macrophages from WT mice, but was not significantly different in those from TIARP$^{-/-}$ mice (Figure 2C). Cleaved caspase 3 levels in the presence of TNFα were clearly diminished in macrophages from TIARP$^{-/-}$ mice as compared to WT mice (Figure 2D). Adding both TNFα and IL-6 induced proliferation in macrophages from TIARP$^{-/-}$ mice as compared to WT mice (data not shown).

Collectively, these results suggested that macrophages from TIARP$^{-/-}$ mice have a high level of response to TNFα due to a weak NF-κB-negative regulation and subsequent proliferation, with dysregulated apoptosis.

**TIARP expression and fluctuation in mice with CIA.** The direct pathogenic effect of TIARP in arthritis was explored using a model of CIA on a B6 background. We first examined TIARP fluctuations in CIA by screening for changes in TIARP expression in WT B6 mice. Real-time quantitative PCR showed up-regulated TIARP mRNA expression on day 23 in splenocytes from mice with CIA and on day 28 in the joints of the same mice, when the expression correlated with joint swelling (Figure 3A). These fluctuations resembled those seen in GPI-induced arthritis (7) and suggest that systemic up-regulation of TNFα and TIARP is involved in the early phases of the disease.

**Exacerbation of CIA in TIARP$^{-/-}$ mice, with increased numbers of antigen-specific Th1 and Th17 cells in LNs, enhanced serum levels of IL-6, and infiltration of macrophages and neutrophils into the joints.** Next, we induced CIA in 8–12-week-old TIARP$^{-/-}$ mice and found exacerbated disease incidence and severity in these mice as compared to the WT mice (Figure 3B). Histologic analysis of TIARP$^{-/-}$ mice with CIA showed marked cell infiltration, pannus formation, and bone erosion, as well as increased histology scores (Figure 3C). Immunohistochemical analysis of cells isolated from the mouse joints confirmed the dominance of neutrophil and macrophage infiltration in the joints of TIARP$^{-/-}$ mice (Figure 3D).

On day 10 after immunization with CII, the TIARP$^{-/-}$ mice had splenomegaly, and their CD4 and CD8 T cell counts were higher than those in WT mice (Figure 4A). In contrast, CD19+ cell counts were not different between WT mice and TIARP$^{-/-}$ mice (data not shown). We then screened T and B cell responses during CIA to investigate antigen-specific responses. The production of antigen-specific cytokines, such as IFNγ and IL-17, was significantly higher in draining LNs from TIARP$^{-/-}$ mice than in those from WT mice (Figure 4B), whereas the numbers of antigen-specific Treg cells (FoxP3+) were not significantly different (Figure 4C). Unexpectedly, the levels of antigen-specific anti-CII antibodies in TIARP$^{-/-}$ mice and WT mice were comparable on day 30 and on day 60 (Figure 4D).

Serum IL-6 levels on day 60 after immunization were also markedly increased in TIARP$^{-/-}$ mice compared to WT mice, whereas TNFα was not detected (Figure 5A). Gene expression analysis in mouse joints on day 60 showed higher levels of IL-6, CXCL2, MMP-3, and RANKL in TIARP$^{-/-}$ mice as compared to WT mice (Figure 5B).

**Suppression of CIA in TIARP$^{-/-}$ mice by anti–IL-6R mAb.** To further confirm the role of IL-6 in arthritis, IL-6 was inhibited after the onset of CIA (on day 21; this timing was generally not effective in WT mice [10]). As anticipated, injection of anti–IL-6R mAb significantly suppressed the incidence and progression of arthritis (Figure 5C, top), and histopathologic analysis on day 60 confirmed this effect (Figure 5C). In contrast, treatment with TNFα-neutralizing antibodies in TIARP$^{-/-}$ mice did not suppress the progression of arthritis (Figure 5C, bottom).

**Enhanced signal in response to IL-6–induced STAT-3 expression in macrophages from TIARP$^{-/-}$ mice.** To further investigate the role of IL-6 signal transduction in TIARP$^{-/-}$ mice, we also measured the expression of pSTAT-3, STAT-3, and SOCS-3 in macrophages. IL-6 stimulation induced STAT-3 and SOCS-3 expression in both groups of mice. However, only pSTAT-3 expression was enhanced in macrophages from TIARP$^{-/-}$ mice as compared to those from WT mice (Figure 5D). In addition, pERK-1/2 production was not changed.

## DISCUSSION

In the present study, we demonstrated that TIARP$^{-/-}$ mice spontaneously develop enthesitis with synovitis and become susceptible to CIA. TIARP is detected during the course of adipocyte differentiation (11) and is also induced by IL-6 (12). TIARP-like proteins such as STEAP-4 are highly expressed in the bone marrow, placenta, and fetal liver (13). In murine hepatocytes, TNFα and IL-17 induce synergistic up-regulation of TIARP (14), and the TIARP gene is a direct target of phosphorylated STAT-3 (15). Recent reports suggest that the expression of 6-transmembrane protein of prostate 2 (STAMP-2)/STEAP-4 in CD14+ macrophages was significantly decreased in women with

metabolic syndrome and correlated with cardiovascular risk (16). The metabolic impact of TIARP has been confirmed in adipocytes from STAMP-2$^{-/-}$ mice (9), but its role in immunity and inflammation remains obscure (17).

Another TNF-induced protein, tumor necrosis factor α–induced protein 3 (TNFAIP-3), has become a particular focus because of its association with RA, as shown in genome-wide association studies (18,19). Matmati et al (20) recently revealed that mice deficient in myeloid-specific TNFAIP-3 spontaneously develop polyarthritis with increased numbers of CD11b+Gr-1+ cells and high levels of inflammatory cytokines (20). This arthritis is clearly dependent on IL-6 (and Toll-like receptor 4), but is independent of TNFα, T cells, and B cells. TIARP (TNFAIP-9) is expressed mainly in macrophages and neutrophils in mice (7) and in humans (8,16) with arthritic conditions, and TIARP$^{-/-}$ mice posses increased numbers of myeloid cells and cytokine dependency similar to that in the conditional TNFAIP-3–deficient mouse model. Thus, the expression of TNF-induced proteins of myeloid origin may be important for the regulation of arthritis via similar pathways.

We found significantly increased numbers of CD11b+Gr-1$^{low/intermediate}$ cells in mouse spleens; thus, we focused mainly on TIARP-dominant cells, such as macrophages, in this study. Stimulation with TNFα or with LPS enhanced the expression of IL-6 in macrophages from TIARP$^{-/-}$ mice. Following TNFα stimulation, sustained degradation of IκBα was noted, and subsequent proliferation with dysregulated apoptosis was seen in macrophages from TIARP$^{-/-}$ mice. Moreover, levels of IL-6–induced pSTAT-3 were also increased in TIARP$^{-/-}$ macrophages, as previously demonstrated in hepatocytes (15).

In addition to macrophages, CD11b+ neutrophils are another cellular source of TIARP/STEAP-4 (7,8). In TIARP$^{-/-}$ mice with CIA, overexpression of CXCL2 (the ligand of CXCR2) in joints was noted, with abundant recruitment of neutrophils. The numbers of CXCR2+ neutrophils were increased in TIARP$^{-/-}$ mice (data not shown), which probably enhanced the severity of the arthritis. In our previous study (8), we confirmed that STEAP-4 transfection of human neutrophils down-regulated their migration. It is possible that overproduction of IL-6 can also augment the adhesion of neutrophils (21).

CIA in the TIARP$^{-/-}$ mice was clearly exacerbated, and IL-6 overproduction was seen. Neutralization of IL-6 during the arthritis induction phase clearly suppressed the arthritis, suggesting a pivotal role of IL-6. The IL-6R-gp130$^{F759}$ mutant mouse is a well-known model of spontaneous arthritis that develops around 12 months of age, with elevated numbers of Gr-1+ CD11b+ cells in LNs (22). In addition to Th17 cells, the importance of IL-6/STAT-3 signals in type I collagen fibroblasts was recently proven in this model (23). TIARP is weakly induced in T cells under arthritic conditions; however, their expression in joint fibroblasts has been confirmed in GPI-induced arthritis (7). STEAP-4 protein was also induced by TNFα in fibroblast-like synoviocytes (FLS), and transfection of STEAP-4 into FLS blocks inflammatory cytokines, such as IL-6 and IL-8, and induces apoptosis (24). Thus, TIARP can regulate innate immune cells and fibroblasts in joints to suppress inflammation and the proliferation that results in suppression of arthritis in an IL-6–related manner.

Taken together, the findings of this study implicate TIARP as a negative regulator of the arthritogenic process through the suppression of IL-6 production, NF-κB, STAT-3 signaling, and the induction of apoptosis. Moreover, systemic deletion of TIARP results in the specific development of RA-like pathology, suggesting that treatment with TIARP or with agents that stimulate TIARP may become an important option for the treatment of RA.

## AUTHOR CONTRIBUTIONS

All authors were involved in drafting the article or revising it critically for important intellectual content, and all authors approved the final version to be published. Dr. Matsumoto had full access to all of the data in the study and takes responsibility for the integrity of the data and the accuracy of the data analysis.

**Study conception and design.** Inoue, Matsumoto, Sumida.

**Acquisition of data.** Inoue, Matsumoto, Yoko Tanaka, Umeda, Yuki Tanaka.

**Analysis and interpretation of data.** Inoue, Matsumoto, Mihara, Takahashi.

## ADDITIONAL DISCLOSURE

Author Mihara is an employee of Chugai Pharmaceutical Company.

## REFERENCES

1. Taylor PC, Feldmann M. Anti-TNF biologic agents: still the therapy of choice for rheumatoid arthritis. Nat Rev Rheumatol 2009;5:578–82.
2. Mima T, Nishimoto N. Clinical value of blocking IL-6 receptor. Curr Opin Rheumatol 2009;21:224–30.
3. Matsumoto I, Staub A, Benoist C, Mathis D. Arthritis provoked by linked T and B recognition of a glycolytic enzyme. Science 1999;286:1732–5.
4. Schubert D, Maier B, Morawietz L, Krenn V, Kamradt T. Immunization with glucose-6-phosphate isomerase induces T cell-dependent peripheral polyarthritis in genetically unaltered mice. J Immunol 2004;172:4503–9.
5. Matsumoto I, Zhang H, Yasukochi T, Iwanami K, Tanaka Y,

Inoue A, et al. Therapeutic effects of antibodies to tumor necrosis factor-α, interleukin-6 and cytotoxic T-lymphocyte antigen 4 immunoglobulin in mice with glucose-6-phosphate isomerase induced arthritis. Arthritis Res Ther 2008;10:R66.
6. Iwanami K, Matsumoto I, Tanaka-Watanabe Y, Inoue A, Mihara M, Ohsugi Y, et al. Crucial role of the interleukin-6/interleukin-17 cytokine axis in the induction of arthritis by glucose-6-phosphate isomerase. Arthritis Rheum 2008;58:754–63.
7. Inoue A, Matsumoto I, Tanaka Y, Iwanami K, Kanamori A, Ochiai N, et al. Tumor necrosis factor α-induced adipose-related protein expression in experimental arthritis and in rheumatoid arthritis. Arthritis Res Ther 2009;11:R118.
8. Tanaka Y, Matsumoto I, Iwanami K, Inoue A, Umeda N, Tanaka Y, et al. Six-transmembrane epithelial antigen of prostate 4 (STEAP4) is expressed on monocytes/neutrophils, and is regulated by TNF antagonist in patients with rheumatoid arthritis. Clin Exp Rheumatol 2012;30:99–102.
9. Wellen KE, Fucho R, Gregor MF, Furuhashi M, Morgan C, Lindstad T, et al. Coordinated regulation of nutrient and inflammatory response by STAMP2 is essential for metabolic homeostasis. Cell 2007;129:537–48.
10. Takagi N, Mihara M, Moriya Y, Nishimoto N, Yoshizaki K, Kishimoto T, et al. Blockage of interleukin-6 receptor ameliorates joint disease in murine collagen-induced arthritis. Arthritis Rheum 1998;41:2117–21.
11. Moldes M, Lasnier F, Gauthereau X, Klein C, Pairault J, Feve B, et al. Tumor necrosis factor-α-induced adipose-related protein (TIARP), a cell-surface protein that is highly induced by tumor necrosis factor-α and adipose conversion. J Biol Chem 2001;276:33938–46.
12. Fasshauer M, Kralisch M, Klier M, Lossner U, Bluher M, Chambaut-Guerin AM, et al. Interleukin-6 is a positive regulator of tumor necrosis factor α-induced adipose-related protein in 3T3-L1 adipocytes. FEBS Lett 2004;560:153–7.
13. Ohgami RS, Campagna DR, McDonald A, Fleming MD. The Steap proteins are metalloreductases. Blood 2006;108:1388–94.
14. Sparna T, Retey J, Schmich K, Albrecht U, Naumann K, Gretz N, et al. Genome-wide comparison between IL-17 and combined TNF-α/IL-17 induced genes in primary murine hepatocytes. BMC Genomics 2010;11:226.
15. Ramadoss P, Chiappini F, Biban M, Hollenberg AN. Regulation of hepatic six transmembrane epithelial antigen of prostate 4 (STEAP4) expression by STAT3 and CCAAT/enhancer-binding protein α. J Biol Chem 2010;285:16453–66.
16. Wang ZH, Zhang W, Gong HP, Guo ZX, Zhao J, Shang YY, et al. Expression of STAMP2 in monocytes associates with cardiovascular alterations. Eur J Clin Invest 2010;40:490–6.
17. Waki H, Tontonoz P. STAMPing out inflammation. Cell 2007;129:451–2.
18. Plenge RM, Cotsapas C, Davies L, Price AL, de Bakker PI, Maller J, et al. Two independent alleles at 6q23 associated with risk of rheumatoid arthritis. Nat Genet 2007;39:1477–82.
19. Thomson W, Barton A, Ke X, Eyre S, Hinks A, Bowes J, et al. Rheumatoid arthritis association at 6q23. Nat Genet 2007;39:1431–3.
20. Matmati M, Jacques P, Maelfait J, Verheugen E, Kool M, Sze M, et al. A20 (TNFAIP3) deficiency in myeloid cells triggers erosive polyarthritis resembling rheumatoid arthritis. Nat Genet 2011;43:908–12.
21. Lally F, Smith E, Filer A, Stone MA, Shaw JS, Nash GB, et al. A novel mechanism of neutrophil recruitment in a coculture model of the rheumatoid synovium. Arthritis Rheum 2005;52:3460–9.
22. Atsumi T, Ishihara K, Kamimura D, Ikushima H, Ohtani T, Hirota S, et al. A point mutation of Tyr-759 in interleukin 6 family cytokine receptor subunit gp130 causes autoimmune arthritis. J Exp Med 2002;196:979–90.
23. Murakami M, Okuyama Y, Ogura H, Asano S, Arima Y, Tsuruoka M, et al. Local microbleeding facilitates IL-6- and IL-17-dependent arthritis in the absence of tissue antigen recognition by activated T cells. J Exp Med 2011;208:103–14.
24. Tanaka Y, Matsumoto I, Iwanami K, Inoue A, Minami R, Umeda N, et al. Six-transmembrane epithelial antigen of prostate 4 (STEAP4) is a tumor necrosis factor α-induced protein that regulates IL-6, IL-8, and cell proliferation in synovium from patients with rheumatoid arthritis. Mod Rheumatol 2012;22:128–36.

ARTHRITIS & RHEUMATISM
Vol. 64, No. 1, January 2012, pp 162–172
DOI 10.1002/art.33335


# Overexpression of T-bet Gene Regulates Murine Autoimmune Arthritis

Yuya Kondo,[1] Mana Iizuka,[1] Ei Wakamatsu,[2] Zhaojin Yao,[1] Masahiro Tahara,[1] Hiroto Tsuboi,[1] Makoto Sugihara,[1] Taichi Hayashi,[1] Keigyou Yoh,[1] Satoru Takahashi,[1] Isao Matsumoto,[1] and Takayuki Sumida[1]

***Objective.*** **To clarify the role of T-bet in the pathogenesis of collagen-induced arthritis (CIA).**

***Methods.*** **T-bet–transgenic (Tg) mice under the control of the CD2 promoter were generated. CIA was induced in T-bet–Tg mice and wild-type C57BL/6 (B6) mice. Levels of type II collagen (CII)–reactive T-bet and retinoic acid receptor–related orphan nuclear receptor γt (RORγt) messenger RNA expression were analyzed by real-time polymerase chain reaction. Criss-cross experiments using CD4+ T cells from B6 and T-bet–Tg mice, as well as CD11c+ splenic dendritic cells (DCs) from B6 and T-bet–Tg mice with CII were performed, and interleukin-17 (IL-17) and interferon-γ (IFNγ) in the supernatants were measured by enzyme-linked immunosorbent assay. CD4+ T cells from B6, T-bet–Tg, or T-bet–Tg/IFNγ$^{-/-}$ mice were cultured for Th17 cell differentiation, then the proportions of cells producing IFNγ and IL-17 were analyzed by fluorescence-activated cell sorting.**

***Results.*** **Unlike the B6 mice, the T-bet–Tg mice did not develop CIA. T-bet–Tg mice showed overexpression of *Tbx21* and down-regulation of *Rorc* in CII-reactive T cells. Criss-cross experiments with CD4+ T cells and splenic DCs showed a significant reduction in IL-17 production by CII-reactive CD4+ T cells in T-bet–Tg mice, even upon coculture with DCs from B6 mice, indicating dysfunction of IL-17–producing CD4+ T cells. Inhibition of Th17 cell differentiation under an in vitro condition favoring Th17 cell differentiation was observed in both T-bet–Tg mice and T-bet–Tg/IFNγ$^{-/-}$ mice.**

***Conclusion.*** **Overexpression of T-bet in T cells suppressed the development of autoimmune arthritis. The regulatory mechanism of arthritis might involve dysfunction of CII-reactive Th17 cell differentiation by overexpression of T-bet via IFNγ-independent pathways.**

Rheumatoid arthritis (RA) is a chronic inflammatory disorder characterized by autoimmunity, infiltration of the joint synovium by activated inflammatory cells, and progressive destruction of cartilage and bone. Although the exact cause of RA is not clear, T cells seem to play a crucial role in the initiation and perpetuation of the chronic inflammation in RA.

The Th1 cell subset has long been considered to play a predominant role in inflammatory arthritis, because T cell clones from RA synovium were found to produce large amounts of interferon-γ (IFNγ) (1). Recently, interleukin-17 (IL-17)–producing Th17 cells have been identified, and this newly discovered T cell population appears to play a critical role in the development of various forms of autoimmune arthritis in experimental animals, such as those with glucose-6-phosphate isomerase–induced arthritis (2) and collagen-induced arthritis (CIA) (3). Conversely, IFNγ has antiinflammatory effects on the development of experimental arthritis (4,5). IL-17 is spontaneously produced by RA synovium (6), and the percentage of IL-17–positive CD4+ T cells

Supported in part by the Japanese Ministry of Science and Culture and by the Japanese Ministry of Health, Labor, and Welfare.

[1]Yuya Kondo, MD, Mana Iizuka, MSc, Zhaojin Yao, MSc, Masahiro Tahara, BSc, Hiroto Tsuboi, MD, PhD, Makoto Sugihara, MD, PhD, Taichi Hayashi, MD, PhD, Keigyou Yoh, MD, PhD, Satoru Takahashi, MD, PhD, Isao Matsumoto, MD, PhD, Takayuki Sumida, MD, PhD: Graduate School of Comprehensive Human Sciences, University of Tsukuba, Tsukuba City, Ibaraki, Japan; [2]Ei Wakamatsu, PhD: Graduate School of Comprehensive Human Sciences, University of Tsukuba, Tsukuba City, Ibaraki, Japan, and Harvard Medical School, Boston, Massachusetts.

Address correspondence to Takayuki Sumida, MD, PhD, Division of Clinical Immunology, Doctoral Programs in Clinical Sciences, Graduate School of Comprehensive Human Science, University of Tsukuba, 1-1-1 Tennodai, Tsukuba City, Ibaraki 305-8575, Japan. E-mail: tsumida@md.tsukuba.ac.jp.

Submitted for publication January 4, 2011; accepted in revised form September 1, 2011.

was increased in the peripheral blood mononuclear cells of patients with RA compared with healthy control subjects (7). It is therefore necessary to determine if autoimmune arthritis is a Th1- or a Th17-associated disorder.

The lineage commitment of each Th cell subset from naive CD4+ T cells is dependent on the expression of specific transcription factors induced under the particular cytokine environment. Differentiation of Th1 cells is dependent on the expression of the transcription factor T-bet, which is induced by IFNγ/STAT-1 signaling pathways and directly activates the production of IFNγ (8,9). Similarly, Th17 cell differentiation in mice is dependent on the transcription factor retinoic acid receptor–related orphan nuclear receptor γt (RORγt) induced by transforming growth factor β (TGFβ) and IL-6 (10). Previous studies showed that these transcription factors negatively regulate the differentiation of other T cell subsets by direct co-interaction and/or indirect effects of cytokines produced from each T cell subset (11,12). How the predominant differentiation of CD4+ T cells affects the development of autoimmune arthritis remains unclear, however.

In the present study, CIA was induced in C57BL/6 (B6) mice and T-bet–transgenic (Tg) mice under the control of the CD2 promoter. The results showed that CIA was significantly suppressed in T-bet–Tg mice as compared with B6 mice. IL-17 production was not detected in type II collagen (CII)–reactive T cells from T-bet–Tg mice, and a significant reduction in IL-17 production by CII-reactive CD4+ T cells from T-bet–Tg mice was observed even when they were cocultured with splenic dendritic cells (DCs) from B6 mice. IFNγ production was also reduced in T-bet–Tg mice as compared with B6 mice, and levels of IFNγ in CII-reactive CD4+ T cells from T-bet–Tg mice were not different from those in B6 mice. Inhibition of Th17 cell differentiation and predominant differentiation of Th1 cells under an in vitro condition favoring Th17 cell differentiation was observed in T-bet–Tg mice, and surprisingly, this inhibition was also observed in T-bet–Tg/IFNγ$^{-/-}$ mice. These results indicate suppression of Th17 cell differentiation by overexpression of T-bet, but not IFNγ. Our findings support the notion that the suppression of autoimmune arthritis in T-bet–Tg mice might be due to the direct inhibition of Th17 cell differentiation by T-bet overexpression in T cells.

## MATERIALS AND METHODS

**Mice.** CD2 T-bet–Tg mice (12) were prepared by backcrossing mice on a C57BL/6 background. IFNγ$^{-/-}$ mice were obtained from The Jackson Laboratory. Littermates of T-bet–Tg mice were used as controls in all experiments. All mice were maintained under specific pathogen–free conditions, and the experiments were conducted in accordance with the institutional ethics guidelines.

**Induction of CIA and assessment of arthritis.** Native chicken CII (Sigma-Aldrich) was dissolved in 0.01*M* acetic acid and emulsified in Freund's complete adjuvant (CFA). CFA was prepared by mixing 5 mg of heat-killed *Mycobacterium tuberculosis* H37Ra (Difco) and 1 ml of Freund's incomplete adjuvant (Sigma-Aldrich). Mice ages 8–10 weeks were injected intradermally at the base of the tail with 200 μg of CII in CFA on days 0 and 21. Arthritis was evaluated visually, and changes in each paw were scored on a scale of 0–3, where 0 = normal, 1 = slight swelling and/or erythema, 2 = pronounced swelling, and 3 = ankylosis. The scores in the 4 limbs were then summed (maximum score 12).

**Histopathologic scoring.** For histologic assessment, mice were killed on day 42 after the first immunization, and both rear limbs were removed. After fixation and decalcification, joint sections were cut and stained with hematoxylin and eosin. Histologic features of arthritis were quantified by 2 independent observers (YK and IM) who were blinded with regard to the study group, and a histologic score was assigned to each joint based on the degree of inflammation and erosion, as described previously (13). The severity of inflammation was scored on a scale of 0–5, where 0 = normal, 1 = minimal inflammatory infiltration, 2 = mild infiltration with no soft tissue edema or synovial lining cell hyperplasia, 3 = moderate infiltration with surrounding soft tissue edema and some synovial lining cell hyperplasia, 4 = marked infiltration, edema, and synovial lining cell hyperplasia, and 5 = severe infiltration with extended soft tissue edema and marked synovial lining cell hyperplasia. The severity of bone erosion was also scored on a scale of 0–5, where 0 = none, 1 = minimal, 2 = mild, 3 = moderate, 4 = marked, and 5 = severe erosion with full-thickness defects in the cortical bone.

**Analysis of cytokine profiles and cytokine and transcriptional factor gene expression.** Inguinal and popliteal lymph nodes were harvested from each mouse on day 10 after the first immunization with CII. Single-cell suspensions were prepared, and lymph node cells ($2 \times 10^5$/well on a 96-well round-bottomed plate) were cultured for 72 hours in RPMI 1640 medium (Sigma-Aldrich) containing 10% fetal bovine serum, 100 units/ml of penicillin, 100 μg/ml of streptomycin, and 50 μ*M* 2-mercaptoethanol in the presence of 100 μg/ml of denatured chicken CII. The supernatants were analyzed for IFNγ, IL-4, IL-10, and IL-17 by enzyme-linked immunosorbent assay (ELISA) using specific Quantikine ELISA kits (R&D Systems).

Lymphocytes harvested on day 10 after immunization were used to obtain complementary DNA (cDNA) by reverse transcription, using a commercially available kit. A TaqMan Assay-on-Demand gene expression product was used for real-time polymerase chain reaction (PCR; Applied Biosystems). The expression levels of *Ifng*, *Il17a*, *Tbx21*, *Rorc*, *Il12a*, and *Il23a* were normalized relative to the expression of *gapdh*. Analyses were performed with an ABI Prism 7500 apparatus (Applied Biosystems).

**Criss-cross coculture with CD4+ T cells and CD11c+ splenic dendritic cells.** Ten days after the first CII immunization, CD4+ cells in draining lymph nodes were isolated by

positive selection, using a magnetic-activated cell sorter (MACS) system with anti-CD4 monoclonal antibody (mAb; Miltenyi Biotec). After treatment with mitomycin C, CD11c+ cells were isolated from the spleen by positive selection, using a MACS system with anti-CD11c mAb (Miltenyi Biotec). Criss-cross coculture for 72 hours was performed with $1 \times 10^5$ CD4+ cells and $2 \times 10^4$ CD11c+ cells in 100 μg/ml of denatured CII-containing medium. Cytokine production and transcription factor expression were then analyzed.

**Measurement of collagen-specific immunoglobulin titers.** Serum was collected from the mice on day 56 after the first immunization. A total of 10 μg/ml of CII in phosphate buffered saline (PBS) was coated overnight at 4°C onto 96-well plates (Nunc MaxiSorp; Nalge Nunc). After washes with washing buffer (0.05% Tween 20 in PBS), the blocking solution, including 1% bovine serum albumin in PBS, was applied for 1 hour. After washing, 100 μl of diluted serum was added, and the plates were incubated for 1 hour at room temperature. After further washing, horseradish peroxidase–conjugated anti-mouse IgG, IgG1, IgG2a, or IgG2b (1:5,000 dilution) in blocking solution was added, and the plates were incubated for 1 hour at room temperature. After washing, tetramethylbenzidine was added, and the optical density was read at 450 nm using a microplate reader.

**Purification of CD4+ cells and in vitro T cell cultures.** CD4+ cells ($1 \times 10^6$/well) were cultured in medium with 1 μg/ml of soluble anti-CD3ε mAb (eBioscience), 1 μg/ml of soluble anti-CD28 mAb (BioLegend), 10 μg/ml of anti-IFNγ mAb (BioLegend), and 10 μg/ml of anti–IL-4 mAb (BioLegend) for a neutral condition. For Th17 cell differentiation, CD4+ cells ($1 \times 10^6$/well) were cultured in medium with 1 μg/ml of soluble anti-CD3ε mAb, 1 μg/ml of soluble anti-CD28 mAb, 3 ng/ml of human TGFβ (R&D Systems), 20 ng/ml of mouse IL-6 (eBioscience), 10 μg/ml of anti-IFNγ mAb, and 10 μg/ml of anti–IL-4 mAb. On day 4, cells were restimulated for 4 hours with 50 ng/ml of phorbol myristate acetate and 500 ng/ml of ionomycin and used in the experiments.

**Surface and intracellular staining and fluorescence-activated cell sorter (FACS) analysis.** GolgiStop (BD PharMingen) was added during the last 6 hours of each culture. Cells were stained extracellularly, fixed, and permeabilized with Cytofix/Cytoperm solution (BD PharMingen). Then, intracellular cytokine staining was performed according to the manufacturer's protocol, using fluorescein isothiocyanate (FITC)–conjugated anti-IFNγ (BD PharMingen) and phycoerythrin (PE)–conjugated anti–IL-17 (BD PharMingen) or FITC-conjugated anti–IL-17 (BioLegend). A Treg cell staining kit (eBioscience) was used to stain T-bet, RORγt, and FoxP3 in cultured cells according to the manufacturer's protocol, using PE-conjugated anti–T-bet (eBioscience), allophycocyanin-conjugated anti-RORγt (eBioscience), and PE-conjugated anti-FoxP3 (eBioscience). Samples were analyzed with a FACSCalibur flow cytometer (Becton Dickinson), and data were analyzed with FlowJo software (Tree Star).

**Statistical analysis.** Data are expressed as the mean ± SEM or the mean ± SD. Differences between groups were examined for statistical significance using Student's *t*-test. *P* values less than 0.05 were considered significant.

## RESULTS

**Construction of the T-bet transgene and tissue distribution of transcription factors and cytokine production in naive mice.** To generate transgenic mouse lines that express high levels of T-bet specifically in T cells, mouse T-bet cDNA was inserted into a VA vector containing a human CD2 transgene cassette (14). To confirm the expression of the transgene, reverse transcription–PCR (RT-PCR) was performed to monitor the expression of *Tbx21* (coding for T-bet) in organs from the T-bet–Tg mice. *Tbx21* messenger RNA (mRNA) expression was detected in the lymphatic system and in nonlymphatic organs in T-bet–Tg mice, and the expression levels were higher than those in B6 mice (data available upon request from the author). Analysis by semiquantitative RT-PCR and quantitative PCR (data not shown) revealed that the expression levels of other transcription factors (*Gata3*, *Rorc*, and *Foxp3*) in T-bet–Tg mice were not different from those in B6 mice. As previously reported by Ishizaki et al (14), high production of IFNγ was observed even when CD4+ T cells isolated from the spleen of T-bet–Tg mice were cultured under neutral conditions (data available upon request from the author).

**Failure to induce CIA and low CII-specific IgG production in T-bet–Tg mice.** To assess whether T cell–specific T-bet expression affects the development of arthritis, we induced CIA in T-bet–Tg mice and in wild-type B6 mice. The incidence and severity of arthritis in T-bet–Tg mice were markedly suppressed compared with those in B6 mice (Figure 1A). Surprisingly, the majority of T-bet–Tg mice were essentially free of arthritis, and even when arthritis was present, it was of the mild type. Consistent with these findings, histologic analyses of the joints obtained from each mouse 42 days after immunization revealed that joint inflammation and destruction were significantly suppressed in T-bet–Tg mice compared with B6 mice (Figures 1B and C). These results indicated that enforced expression of T-bet in T cells suppressed the development of CIA.

Because the levels of CII-specific IgG correlate well with the development of arthritis (15), we examined CII-specific IgG production in T-bet–Tg mice. CII-specific IgG, IgG1, IgG2a, and IgG2b levels were significantly lower in T-bet–Tg mice than in B6 mice, as determined by ELISA (Figure 1D). Thus, enforced expression of T-bet in T cells suppresses the development of CIA and CII-specific IgG production.

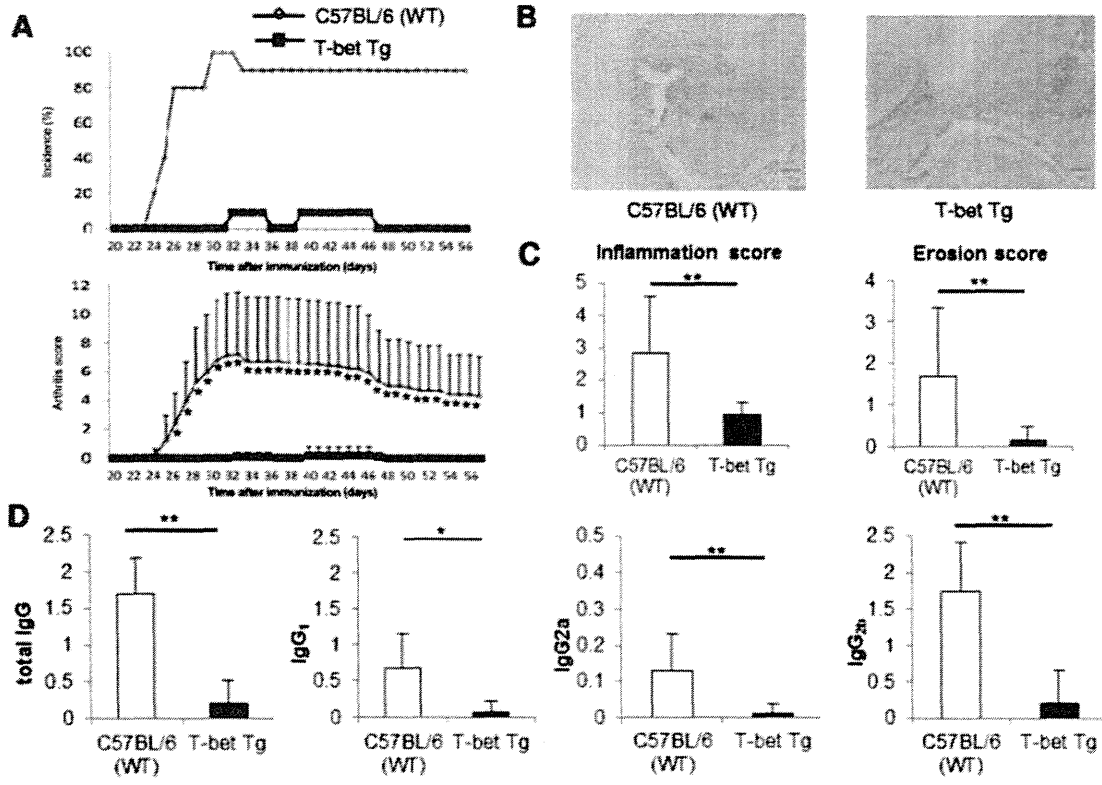


**Figure 1.** Significant suppression of collagen-induced arthritis (CIA) and type II collagen (CII)–specific IgG production in T-bet–transgenic (Tg) mice. On days 0 and 21, mice were immunized intradermally at several sites at the base of the tail with chicken CII emulsified with Freund's complete adjuvant. **A,** Incidence and severity of CIA. The arthritis score was determined as described in Materials and Methods. Data were obtained from 2 independent experiments involving 10 C57BL/6 (wild-type [WT]) mice and 11 T-bet–Tg mice. **B,** Hematoxylin and eosin–stained sections of the hind paws of mice obtained 6 weeks after the first immunization. Original magnification × 40. **C,** Inflammation and bone erosion scores in 7 C57BL/6 mice and 5 T-bet–Tg mice 6 weeks after the first immunization. Scores were determined as described in Materials and Methods. **D,** Serum levels of CII-specific IgG, IgG1, IgG2a, and IgG2b levels in 10 C57BL/6 mice and 11 T-bet–Tg mice 8 weeks after the first immunization, as measured by enzyme-linked immunosorbent assay. Values in **A, C,** and **D** are the mean ± SD. * = $P < 0.05$; ** = $P < 0.01$ by Student's *t*-test.

**Suppression of CII-reactive IL-17 production and IL-17 mRNA expression in T-bet–Tg mice.** Because enforced T-bet expression in T cells suppressed the development CIA, we examined antigen-specific cytokine production and transcription factor expression in mice with CIA. CD4+ T cells harvested from draining lymph nodes were stimulated with CII in vitro, and then various cytokine levels in the supernatants were measured by ELISA. IL-17 production by CII-reactive T cells was significantly reduced in T-bet–Tg mice as compared with B6 mice (Figure 2A). IFNγ production by CII-reactive T cells also tended to be decreased in T-bet–Tg mice.

We analyzed CII-reactive cytokine and transcription factor mRNA expression levels by real-time PCR (Figure 2B). Similar to the ELISA results, *Il17a* expression tended to be lower in T-bet–Tg mice than in B6 mice. No difference in *Ifng* expression was observed between B6 and T-bet–Tg mice (Figure 2B). *Tbx21* expression tended to be higher in T-bet–Tg mice, whereas *Rorc* expression was lower in T-bet–Tg mice than in B6 mice ($P < 0.05$). The level of expression of *Il12a* (coding for IL-12p35) was also higher in T-bet–Tg mice than in B6 mice ($P < 0.05$). However, there was no difference in the expression levels of *Il23a* (coding for IL-23p19) between B6 mice and T-bet–Tg mice. These

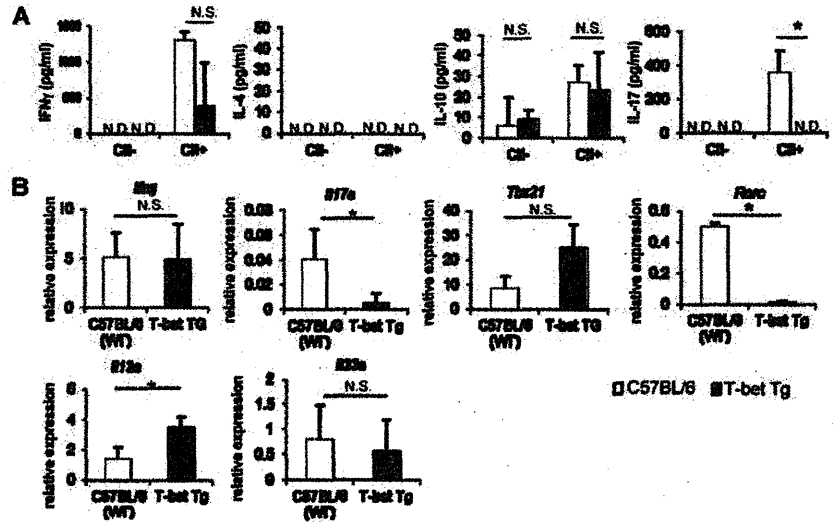


**Figure 2.** No production of interleukin-17 (IL-17) and low production of interferon-γ (IFNγ) in type II collagen (CII)–reactive CD4+ T cells. **A,** Ten days after the first CII immunization, lymphocytes derived from the draining lymph nodes of C57BL/6 (wild-type [WT]) mice and T-bet–transgenic (Tg) mice were cultured for 72 hours in the presence or absence of 100 μg/ml of denatured CII. Levels of IL-17, IFNγ, IL-4, and IL-10 in the supernatants were measured by enzyme-linked immunosorbent assay. **B,** After culture of lymphocytes with CII, cDNA was obtained, and levels of *Ifng*, *Il17a*, *Tbx21*, *Rorc*, *Il12a*, and *Il23a* expression were analyzed by real-time polymerase chain reaction. Values are the mean ± SD of 3 mice. * = $P < 0.05$ by Student's *t*-test. ND = not detected; NS = not significant.

results suggest that overexpression of T-bet on CD4+ T cells suppressed the expression of RORγt and IL-17.

**No reduction of RORγt expression on CII-reactive CD4+ T cells in T-bet–Tg mice.** CD4+ T cells from T-bet–Tg and B6 mice were cultured in vitro with CII, and analyses of T-bet and RORγt expression on CD4+ T cells were carried out by the intracellular staining method. T-bet expression on CII-reactive CD4+ T cells was significantly higher in T-bet–Tg mice than in B6 mice (Figure 3A). Surprisingly, the majority of T-bet+ CII-reactive T cells expressed RORγt in both the B6 mice and the T-bet–Tg mice (Figure 3A). Although there was no significant difference in the mean fluorescence intensity of RORγt between B6 mice and T-bet–Tg mice, the number of RORγt+ cells tended to be lower in T-bet–Tg mice (data available upon request from the author).

Moreover, in the case of CD4+ T cells examined under conditions favoring Th17 differentiation, RORγt expression on CD4+ T cells from T-bet–Tg mice was lower than that on cells from B6 mice (Figure 3B). Interestingly, most of the RORγt+ cells also expressed T-bet in the T-bet–Tg mice, and the proportion of IL-17–producing RORγt+ CD4+ T cells was lower in the T-bet–Tg mice than in the B6 mice. These findings support the notion that overexpression of T-bet not only suppresses RORγt expression on CD4+ T cells but also inhibits the production of IL-17 from RORγt+ T cells.

To investigate whether the suppression of arthritis and low antigen-specific cytokine production observed in T-bet–Tg mice was related to Treg cells, the next experiment analyzed FoxP3 expression on CD4+ T cells harvested from draining lymph nodes 10 days after immunization. There was no significant difference in the percentage of FoxP3+ cells among the CD4+ T cells between B6 mice and T-bet–Tg mice (data available upon request from the author). Thus, Treg cells do not seem to be involved in the suppression of CIA in T-bet–Tg mice.

**Decreased numbers of T cells in the lymph nodes, spleen, and thymus of T-bet–Tg mice.** To evaluate the low cytokine response and the low population of CII-reactive RORγt+CD4+ T cells in T-bet–Tg mice with CIA, we analyzed the lymphocyte subsets in the draining lymph nodes and spleen after immunization. The percentage and absolute number of CD3+ T cells were lower in both the draining lymph nodes and the